

1 For publication in Journal of Virology  
2

3 **Mutations in a highly conserved motif of nsp1 $\beta$  protein attenuate the innate immune**  
4 **suppression function of porcine reproductive and respiratory syndrome virus (PRRSV)**  
5

6 *Yanhua Li<sup>1a</sup>, Duan-Liang Shyu<sup>2a</sup>, Pengcheng Shang<sup>1</sup>, Jianfa Bai<sup>1</sup>, Kang Ouyang<sup>2</sup>, Santosh*  
7 *Dhakai<sup>2</sup>, Jagadish Hireamt<sup>2</sup>, Basavaraj Binjawadagi<sup>2</sup>, Gourapura J. Renukaradhya<sup>2\*</sup>, Ying*  
8 *Fang<sup>1\*</sup>*  
9

10 1. Department of Diagnostic Medicine and Pathobiology, College of Veterinary Medicine,  
11 Kansas State University, Manhattan, KS 66506.

12 2. Food Animal Health Research Program (FAHRP), Veterinary Preventive Medicine, The Ohio  
13 State University, Wooster, OH 44691.

14  
15  
16 \*To whom correspondence should be addressed. E-mail: [gourapura.1@osu.edu](mailto:gourapura.1@osu.edu); [yfang@vet.k-](mailto:yfang@vet.k-state.edu)  
17 [state.edu](mailto:yfang@vet.k-state.edu).

18  
19  
20 <sup>a</sup>Yanhua Li and Duan-Liang Shyu contribute equally to this work.  
21

22 Running title: PRRSV nsp1 $\beta$  mutation and attenuation *in vivo*  
23

24 Abstract word count: 250

25 Main text word count: 9933  
26

27 **ABSTRACT**

28 PRRSV nonstructural protein 1 $\beta$  (nsp1 $\beta$ ) is a multifunctional viral protein, which involves in  
29 suppressing innate immune response and activating a unique -2/-1 programmed ribosomal  
30 frameshifting (PRF) signal for the expression of frameshifting products. In this study, site-  
31 directed mutagenesis analysis showed that R128A or R129A mutation introduced in a highly  
32 conserved motif (<sub>123</sub>GKYLQRRLQ<sub>131</sub>) reduced the ability of nsp1 $\beta$  to suppress IFN- $\beta$  activation  
33 and also impaired nsp1 $\beta$ 's function as PRF transactivator. Three recombinant viruses, vR128A,  
34 vR129A and vRR129AA, carrying single or double mutations in the GKYLQRRLQ motif were  
35 characterized. In comparison to the wild type (WT) virus, vR128A and vR129A showed slightly  
36 reduced growth ability, while vRR129AA mutant had significantly reduced growth ability in  
37 infected cells. Consistent with the attenuated growth phenotype *in vitro*, the pigs infected with  
38 nsp1 $\beta$  mutants had lower level of viremia than that of WT virus-infected pigs. Comparing to WT  
39 virus in infected cells, all of the three mutated viruses stimulated higher level of IFN- $\alpha$   
40 expression and exhibited reduced ability in suppressing mRNA expression of selected ISGs. In  
41 pigs infected with nsp1 $\beta$  mutants, IFN- $\alpha$  production was increased in the lungs during early time  
42 points of post-infection, which was correlated with an increased innate NK cell function.  
43 Furthermore, augmented innate response was consistent with increased production of IFN- $\gamma$  in  
44 those mutated viruses-infected pigs. These data demonstrate that R128 and R129 residues are  
45 critical for nsp1 $\beta$  function, and modifying these key residues in the GKYLQRRLQ motif  
46 attenuates virus growth ability and improve the innate and adaptive immune responses in  
47 infected animals.

48

49

50 **IMPORTANCE**

51 PRRSV infection induces poor anti-viral innate IFN and cytokine responses, which results in  
52 weak adaptive immunity. One of the strategies in next generation vaccine construction is to  
53 manipulate viral proteins/genetic elements involved in antagonizing host immune response. The  
54 PRRSV nsp1 $\beta$  was identified to be a strong innate immune antagonist. In this study, two basic  
55 amino acids, R128 and R129, in a highly conserved GKYLQRRLQ motif were determined to be  
56 critical for nsp1 $\beta$  function. Mutations introduced into these two residues attenuated virus growth  
57 and improved the innate and adaptive immune responses in infected animals. Technologies  
58 developed in this study could be broadly applied to current commercial PRRSV MLV vaccines  
59 and other candidate vaccines.

60

61

## 62 INTRODUCTION

63 Porcine reproductive and respiratory syndrome (PRRS), a disease described in the US in 1987  
64 (1) and in Europe in 1990 (2), has caused tremendous economic losses to the swine industry  
65 since its appearance. Hallmark symptoms of PRRS are mild to severe respiratory disease in  
66 infected newborn and growing pigs, and reproductive failure in pregnant sows. The etiologic  
67 agent, PRRS virus (PRRSV), was first discovered in the Netherlands in 1991 (2). In the US,  
68 PRRSV was first isolated and characterized in 1992 (3, 4). Generally, infection of pigs by most  
69 of the PRRSV strains dampens the host innate immune response (5, 6). This initial suppression  
70 of host innate immune response, leading to the delayed induction of protective cellular and  
71 humoral immunity (7, 8), which provides a window of time that allows PRRSV to replicate, shed  
72 and transmit to other contact naïve animals. Therefore, strategies for vaccine development are  
73 directed at constructing a PRRS vaccine capable of inducing a high level of innate and adaptive  
74 immune responses.

75 PRRSV is an enveloped, positive-stranded RNA virus, which belongs to the order *Nidovirales*,  
76 family *Arteriviridae*, including equine arteritis virus (EAV), mouse lactate dehydrogenase-  
77 elevating virus (LDV), simian hemorrhagic fever virus (SHFV) and several recently discovered  
78 monkey arteriviruses that are only distantly related to SHFV (9). The PRRSV genome is about  
79 15kb in length and contains at least eleven open reading frames. The 3' end of the genome  
80 encodes four membrane-associated glycoproteins (GP2a, GP3, GP4 and GP5), three  
81 unglycosylated membrane proteins (E, ORF5a and M) and a nucleocapsid protein (N) (10-19).  
82 The replicase-associated genes, ORF1a and ORF1b, situated at the 5' end, and represent nearly  
83 75% of the viral genome. The ORF1a and ORF1b encode two large polyproteins, pp1a and  
84 pp1ab, with expression of the latter depending on a -1 ribosomal frameshifting signal in the

85 ORF1a/ORF1b overlap region. Following their synthesis from the genomic mRNA template, the  
86 pp1a and pp1ab replicase polyproteins are processed into at least 14 nonstructural proteins (nsps)  
87 by a complex proteolytic cascade that is directed by four proteinase domains encoded in ORF1a,  
88 which include two papain-like proteinases (PLP1 $\alpha$  and PLP1 $\beta$ ) located in the nsp1 $\alpha$  and nsp1 $\beta$ , a  
89 papain-like proteinase (PLP2) domain located at the N-terminal of nsp2, and a serine proteinase  
90 located in nsp4. The PLP $\alpha$  auto-cleaves between nsp1 $\alpha$ /1 $\beta$ , PLP $\beta$  auto-cleaves between nsp1 $\beta$ /2,  
91 and PLP2 cleaves between nsp2/3, which mediate the rapid release of nsp1 $\alpha$ , nsp1 $\beta$  and nsp2  
92 from the polyprotein (20). Recently, two novel PRRSV proteins, nsp2TF and nsp2N, were  
93 identified (21). The nsp2TF and nsp2N are expressed by a novel -2/-1 programmed ribosomal  
94 frameshifting (PRF) mechanism, which accesses the alternative ORF (TF) through a  
95 frameshifting site that overlaps the nsp2-encoding region. Both nsp2TF and nsp2N share the N-  
96 terminal 2/3 sequence with nsp2, which contains the PLP2 domain.

97 Previous studies from our laboratory and others identified PRRSV nsp1 $\beta$  to be a strong innate  
98 immune antagonist (22-24). PRRSV nsp1 $\beta$  has strong inhibitory effects on type I IFN production  
99 and signaling pathways that lead to the expression of interferon stimulated genes (ISGs).  
100 Interestingly, this protein was recently identified to also function as a transactivator for the  
101 expression of -2/-1 PRF products, nsp2TF and nsp2N (25). Embedded in nsp1 $\beta$ 's papain-like  
102 autoprotease domain (PLP1 $\beta$ ), a highly conserved GKYLQRRLQ motif was identified to be  
103 critical for -2/-1 PRF transactivation and innate immune suppression function of the virus (25,  
104 26). Based on the crystal structure analysis, three basic residues (K124, R128, and R129) in  
105 GKYLQRRLQ motif are exposed on the surface of the protein (25). In this study, we further  
106 investigated the function of the basic residues K124, R128, and R129 involved in modulation of

107 host immune responses. Recombinant viruses carrying mutations in these basic residues were  
108 created and characterized in cell culture systems as well as in a nursery piglet model.

109

## 110 MATERIALS AND METHODS

111 Cells and viruses. HEK-293T cells and MARC-145 cells were maintained in minimum essential  
112 medium (Gibco) supplemented with 10% fetal bovine serum and antibiotic (Streptomycin, 100  
113  $\mu\text{g}/\text{mL}$ ) at 37 °C with 5% CO<sub>2</sub>. BHK-21 cells were cultured in minimum essential medium  
114 supplemented with 5% fetal bovine serum and antibiotic (Streptomycin, 100  $\mu\text{g}/\text{mL}$ ). As  
115 described previously, porcine alveolar macrophages were obtained from lung lavage of 6-week-  
116 old PRRSV naive piglets (27). The Sendai virus (SeV), Cantell strain, grown in embryonated  
117 chicken eggs was used for stimulation of type 1 IFN response in cell culture system. The type 2  
118 PRRSV isolate SD95-21 (GenBank accession: KC469618), and its nsp1 $\beta$  mutants were used for  
119 subsequent experiments.

120 Antibodies. To detect the expression of nsp1 $\beta$  and its mutants, mAb 123-128 (25) or the anti-  
121 FLAG M2 mAb (Sigma-Aldrich, St. Louis, MO) was used. The mAb 140-68 (25), specifically  
122 recognizing the common N-terminal PLP2 domain of nsp2, nsp2TF and nsp2N, was used to  
123 detect the expression of nsp2-related proteins. The rabbit pAb against nsp2TF (25) was utilized  
124 to immunoprecipitate and detect nsp2TF. In addition, the anti- $\beta$ -tubulin mAb (abm Inc., BC,  
125 Canada) was used to detect the expression of housekeeping gene  $\beta$ -tubulin. Antibody mixture of  
126 mAb M2 against FLAG and anti- $\beta$ -tubulin was used for simultaneously detection the expression  
127 of FLAG-tagged nsp1 $\beta$  and  $\beta$ -tubulin in western blot, while antibody mixture of mAb 123-128  
128 and anti- $\beta$ -tubulin was used for simultaneously detection the expression of nsp1 $\beta$  and  $\beta$ -tubulin  
129 in western blot.

130 Plasmids. Using the nsp1 $\beta$  expressing plasmid (p3xFLAG-NA-nsp1 $\beta$ ) that we generated  
131 previously (26), specific mutations, K124A, R128A, R129A, or RR129AA (double mutations of  
132 R128A and R129A) in the GKYLQRRLQ motif region (amino acids 123-131) of nsp1 $\beta$  were  
133 introduced by site-directed mutagenesis using QuickChange<sup>TM</sup> site-directed mutagenesis kit  
134 (Agilent Technologies, Inc., Santa Clara, CA), following the manufacturer's instruction. A  
135 vaccinia/T7 polymerase system (pL-NA-nsp1 $\beta$ -2) expressing the nsp1 $\beta$ -nsp2 of SD95-21 virus  
136 was described previously (26). Specific mutations (K124A, R128A, R129A, or RR129AA) were  
137 introduced into the nsp1 $\beta$  region of pL-NA-nsp1 $\beta$ -2 using QuickChange<sup>TM</sup> site-directed  
138 mutagenesis kit. To generate full-length PRRSV cDNA clones containing these specific  
139 mutations (R128A, R129A, or RR129AA), a shuttle plasmid carrying the region between two  
140 unique restriction sites (*Sph I* and *Sca I*) of the full-length cDNA clone of PRRSV (pCMV-  
141 SD95-21) was constructed using Zero Blunt<sup>®</sup> PCR Cloning Kit (Invitrogen, Carlsbad, CA).  
142 QuickChange<sup>TM</sup> site-directed mutagenesis kit (Agilent Technologies, Inc., Santa Clara, CA) was  
143 employed to introduce the specific mutations into the shuttle plasmid. The region between *Sph I*  
144 and *Sca I* of pCMV-SD95-21 was replaced by the corresponding regions of the shuttle plasmids  
145 containing the specific mutations. The mutated full-length cDNA clones were designated as  
146 pCMV-SD95-21-R128A, pCMV-SD95-21-R129A, and pCMV-SD95-21-RR129AA. DNA  
147 sequencing was further performed to verify the introduced mutations. For *in vitro* luciferase  
148 reporter assay, two reporter plasmids, the p125-Luc and pISRE-Luc, were used as described  
149 previously (26).

150 Luciferase reporter assay. HEK-293T cells were seeded at  $0.5 \times 10^5$  cells/mL in 24-well plates  
151 one day before transfection. DNA transfection was conducted using FuGENE HD transfection  
152 reagent (Promega, Madison, WI). Briefly, cells were co-transfected with 0.5  $\mu$ g plasmid DNA

153 expressing WT nsp1 $\beta$  (or its mutants) and 0.5  $\mu$ g luciferase reporter plasmid DNA of p125-Luc  
154 or pISRE-Luc. At 24 h post-transfection, cells were mock treated or stimulated with the SeV  
155 inoculated at 100 HA unit/ml/well for 16 h, or treatment with IFN- $\beta$  at 2000 IU/ml/well for 16 h.  
156 Cells were lysed and used for reporter gene assay using the dual luciferase reporter system  
157 (Promega, Madison, WI) according to the manufacturer's instruction. Firefly luciferase activities  
158 were measured with FLUOstar Omega (BMG LABTECH, Cary, NC).

159 *Vaccinia/T7 polymerase expression system.* The nsp1 $\beta$ -nsp2 and its mutants were expressed  
160 using a vaccinia/T7 polymerase system (28) as described previously (26). Briefly, HEK-293T  
161 cells (1x10<sup>6</sup>/well) were seeded in 6-well plates one day before infection. Cells in each of the well  
162 were infected with a vaccinia virus expressing T7 polymerase at a multiplicity of infection (MOI)  
163 of 10. At 1 h post-infection, cells were transfected with 2 $\mu$ g DNA of pL-NA-nsp1 $\beta$ -2 or its  
164 mutants using FuGENE HD transfection reagent (Promega, Madison, WI). At 18 h post-  
165 transfection, cell lysate from each well of 6-well plate was harvested and subjected to western  
166 blot analysis using antibodies against nsp1 $\beta$  (mAb 123-128) and nsp2 (mAb 140-68). In addition,  
167 cell lysate was used in immunoprecipitation to evaluate the expression of -2 PRF product with  
168 the antibody that specifically recognizes nsp2TF (pAb-TF).

169 *Western Blot Analysis.* Western blot analysis was performed to evaluate protein expression using  
170 the method described previously (20, 26). Briefly, cell lysates were prepared by harvesting virus-  
171 infected or plasmid DNA-transfected cells with RIPA buffer. Cell lysate was mixed with equal  
172 volume of Laemmli sample buffer and heated at 95  $^{\circ}$ C for 6 min. After being separated by  
173 sodium dodecyl sulfate-polyacrylamide gel electrophoresis (SDS-PAGE), proteins were  
174 transferred onto a nitrocellulose membrane. The membrane was blocked with 5% skim milk in  
175 PBST (PBS with 0.05% Tween 20) at 4  $^{\circ}$ C overnight, and then incubated with primary antibody



176 at appropriate dilution at room temperature for 1h. After 3 times wash with PBST, the secondary  
177 antibody, IRDye® 800CW Goat anti-Mouse IgG (H + L) or/and IRDye® 680RD Goat anti-  
178 Rabbit IgG (H + L) (LI-COR Biosciences, Lincoln, NE), was added and the membrane was  
179 incubated for additional 1 h at room temperature. The target proteins were visualized and  
180 quantified using a digital image system (Odyssey infrared imaging system; LI-COR Biosciences,  
181 Lincoln, NE). For quantification of the target proteins, the expression levels were normalized to  
182 the expression level of  $\beta$ -tubulin, which is a house keeping gene used as a loading control.

183 Recovery of recombinant viruses from infectious cDNA clones. The procedure for generating  
184 recombinant viruses was described previously (26). BHK-21 cells with 70-80% confluency were  
185 transfected with 2  $\mu$ g of the type 2 PRRSV full-length cDNA clone of pCMV-SD95-21 or the  
186 full-length cDNA clones containing nsp1 $\beta$  mutations. Transfection was performed using  
187 FuGENE HD reagent (Promega, Madison, WI). At 48 h post-transfection, cell culture  
188 supernatant was harvested and passaged onto MARC-145 cells. After 48-60 h of incubation,  
189 indirect immunofluorescence assay were performed to confirm the viability of recombinant  
190 viruses using mAb SDOW17 (PRRSV N protein-specific monoclonal antibody, (29)). The  
191 recombinant viruses were serially passaged on MARC-145 cells, and passage 3 and 4 viruses  
192 were used for further analysis.

193 Sequencing of nsp1 $\beta$  mutation regions. To determine the stability of each mutation, cell culture  
194 supernatant from recombinant virus-infected cells or serum samples collected from  
195 experimentally infected animals [14, 21 and 35 days post infection (DPI)] were used for viral  
196 RNA extraction using the QIAamp viral RNA kit (QIAGEN). The nsp1 $\beta$  coding region  
197 containing the corresponding mutations was amplified by RT-PCR, and PCR products were  
198 subjected to DNA sequencing at GENEWIZ, Inc. (South Plainfield, NJ).

199 Virus growth kinetics and plaque assay. The passage 3 of WT and mutant viruses were used to  
200 characterize viral growth properties *in vitro*. Confluent MARC-145 cells were inoculated with  
201 WT virus or nsp1 $\beta$  mutants at a MOI of 0.01. Cell culture supernatant was harvested at 12, 24,  
202 36, 48, 60, 72 h post-infection. Virus titer was measured by micro-titration assay using MARC-  
203 145 cells in 96-well plates and calculated as TCID<sub>50</sub>/ml according to the Reed and Muench  
204 method (30). To determine the plaque morphology of WT virus and nsp1 $\beta$  mutants, plaque assay  
205 was conducted using MARC-145 cells as described previously (31).

206 Pig groups, sample collection and preparation. A total of 45 specific pathogen free (SPF) pigs  
207 were obtained from the swine farm of The Ohio State University. Pigs were randomly divided  
208 into 5 groups (n=9; Table 1). Pigs were mock-infected (group 1), or infected with 4x10<sup>6</sup> TCID<sub>50</sub>  
209 of WT PRRSV (group 2), vR128A mutant (group 3), vR129A mutant (group 4), vRR129AA  
210 mutant (group 5). The virus was inoculated through both intranasal (IN) and intramuscular (IM)  
211 routes with 1mL (1x10<sup>6</sup> TCID<sub>50</sub>) of the virus suspension in MEM to each nostril and to each side  
212 of the neck. Pigs were observed daily and blood samples were collected on 0, 1, 2, 5, 7, 14, 21,  
213 28, 35 DPI. Three pigs from each group were sequentially euthanized at 7, 21, and 35 DPI (Table  
214 1). During necropsy, the lungs were evaluated for gross lesions using the method described  
215 previously (32), and bronchoalveolar lavage fluid (BALF) and lung tissue samples were  
216 collected as described previously (33). The pig experiment was performed according to the  
217 protocol approved by the Institutional Animal Care and Use Committee (IACUC) of The Ohio  
218 State University, Ohio.

219 Real-time RT-PCR quantification of viral load in infected animals. For the determination of viral  
220 RNA load, serum, BALF and lung lysate samples were examined using a real-time quantitative  
221 RT-PCR. Briefly, viral genomic RNA was extracted using MagMAX™-96 viral RNA isolation

222 kit (life technologies) following the manufacturer's instruction. Viral RNA level was determined  
223 by a quantitative RT-PCR using iTaq™ Universal SYBR® Green One-Step Kit (Bio-Rad,  
224 Hercules, CA), and the RNA copy numbers were calculated based on a RNA standard curve. A  
225 pair of primers, PRRS-qF1 (CCATTTCCCTTGACACAGTCG) and PRRS21-qR2  
226 (GACCGCGTAGATGCTACTTAGG) located at viral genomic region (nt 14043-14130), was  
227 designed for the real-time RT-PCR. The RNA standard was prepared by *in vitro* transcription.  
228 Briefly, the viral genomic region (nt 13918-14246) was amplified by RT-PCR using primer pairs,  
229 T7-GP5F (TCTAGATAATACGACTCACTATAGGGAACTTGACGCTATGTGAGCTG,  
230 underline indicates T7 promoter) and GP5R (TAGAGTCTGCCCTTAGTGTCCA). PCR product  
231 was purified and subjected to *in vitro* transcription using MEGAscript® T7 Transcription Kit  
232 (Invitrogen, Carlsbad, CA). The purified RNA product was used as the quantification standard.

233 Quantitative analysis of mRNA. Porcine alveolar macrophages were infected with WT virus or  
234 nsp1β mutants at a MOI of 1. At 12 h post-infection, PAMs were harvested with TRIzol LS  
235 (Ambion, Foster City, CA) and subjected to total RNA extraction according to the  
236 manufacturer's instruction. After removing contaminating genomic DNA with TURBO DNA-  
237 free™ Kit (Invitrogen, Carlsbad, CA), 1 μg total RNA was used to synthesize first-strand cDNA  
238 using SuperScript® VILO™ cDNA Synthesis Kit (Invitrogen, Carlsbad, CA). Subsequently,  
239 real-time PCR was performed to quantify the expression of mRNA of ISG15, IFIT1, IFITM1 and  
240 β-tubulin using predesigned primer/probe sets (Applied Biosystems, Foster City, CA), following  
241 the manufacturer's instruction. The amount of ISG15, IFIT1 and IFITM1 mRNA was normalized  
242 to the endogenous β-tubulin mRNA.

243 Analysis of swine cytokine response. Porcine alveolar macrophages were infected with WT virus  
244 or nsp1β mutants at a MOI of 1. At 12 h post-infection, cell culture supernatant was harvested

245 for analyzing the IFN- $\alpha$  expression using ProcartaPlex Porcine IFN alpha Simplex kit  
246 (eBioscience, San Diego, CA). In addition, Serum, BALF and lung lysate samples were used for  
247 measuring the levels of secreted cytokines, IFN- $\alpha$ , IFN- $\gamma$ , IL-6, and IL-10 by ELISA as described  
248 previously (34).

249 Pig NK cell cytotoxic assay. To determine the pig NK cell-mediated cytotoxicity, the  
250 immunofluorescence based assay was performed using a modified method described previously  
251 (34-36). The assay was conducted using the 7-AAD/CFSE cell-mediated cytotoxicity assay kit  
252 (Cayman Chemical, Ann Arbor, MI). Briefly, PBMCs isolated from pigs were used as the source  
253 of NK cells (effectors) against K562 (human myeloblastoid cell line) target cells. The target cells  
254 were labeled with CFSE according to the manufacturer's recommendation. Effector and target  
255 cells were incubated at different E:T ratios at 37<sup>o</sup> C overnight. The frequency of apoptotic CFSE-  
256 labeled K562 cells that were mediated by NK cells was measured by staining the co-cultured  
257 target cells with the 7-AAD nuclear dye. The specific NK cell-cytotoxicity was measured using  
258 flow cytometry by acquiring 10,000 CFSE labeled events, and further gated for CFSE and 7ADD  
259 (green and red) double staining cell frequency, which indicates the NK-lysed cell frequency.  
260 Appropriate controls include K562 cells labeled or unlabeled with CFSE, and apoptosis induced  
261 K562 cells (treated with UV at 254nm for 30 min and then incubated for 6-8 h at 37 °C). The  
262 percentage of NK-specific lysis was calculated using the formulae: double positive K562  
263 cells/CFSE positive cells multiplied by 100.

264 Flow cytometry analysis. Immunophenotyping of PBMCs was performed as previously  
265 described (33, 37). Briefly, PBMCs were first surface-labeled with pig lymphocyte specific  
266 fluorochrome-conjugated mAbs (CD3 $\epsilon$ -PerCP, CD4 $\alpha$ -APC and CD8 $\alpha$ -FITC). For intracellular  
267 IFN- $\gamma$  staining, GolgiPlug<sup>TM</sup> (BD Biosciences, San Jose, CA, USA) and Brefeldin A (B7651,

268 Sigma-Aldrich, St. Louis, MO) were added during the last 12 h of incubation of PBMCs treated  
269 with or without the respective virus as a stimulant at a MOI of 1. The surface immunostained  
270 cells were fixed with 1% paraformaldehyde and permeabilized with a cell-permeabilization  
271 buffer (85.9% deionized water, 11% PBS without  $\text{Ca}^{2+}$  or  $\text{Mg}^{2+}$ , 3% formaldehyde solution, and  
272 0.1% saponin) overnight at 4°C. Cells were washed and stained with fluorochrome-conjugated  
273 anti-pig IFN- $\gamma$  or its isotype control mAb (BD Biosciences, East Rutherford, NJ) in 0.1%  
274 saponin containing fluorescence-activated cell-sorting (FACS) buffer. Immunostained cells were  
275 acquired using the FACS Aria II (BD Biosciences, East Rutherford, NJ) flow cytometer and  
276 analyzed using FlowJo (Tree Star, Ashland, OR, USA) software. All specific cell population  
277 frequencies were presented as the percentage of lymphocytes in PBMCs.

278 Statistical analysis. All the data were expressed as the mean of 3 to 9 pigs  $\pm$  standard error of the  
279 mean (SEM). Statistical analyses were performed using one way analysis of variance (ANOVA)  
280 followed by post-hoc Tukey's test using GraphPad InStat Prism (software version 5.0) to  
281 establish variations between indicated pig groups. Statistical significance was assessed at  $P < 0.05$   
282 (\*),  $P < 0.01$  (\*\*),  $P < 0.001$  (\*\*\*)).

283

## 284 RESULTS

### 285 Identification of critical residues on GKYLQRRLQ motif for PRRSV nsp1 $\beta$ function

286 In our previous study (26), we identified a highly conserved GKYLQRRLQ motif in PRRSV  
287 nsp1 $\beta$  that is critical for the innate immune suppression function of this protein. Protein  
288 structural analysis showed that three basic residues (K124, R128, and R129) in GKYLQRRLQ  
289 motif are exposed on the surface of nsp1 $\beta$  (25). In this study, we further investigated the function  
290 of these three basic residues. A panel of nsp1 $\beta$  mutants was generated. Each of the nsp1 $\beta$  genes

291 carries a single alanine substitution at amino acid K124 (K124A), R128 (R128A), R129 (R129A)  
292 or double alanine substitutions at R128/R129 (RR129AA). A previously created mutant  
293 nsp1 $\beta$ KO (R124/R128 to A124/A128 double substitutions (26)) was also included in the  
294 analysis. These nsp1 $\beta$  mutants were cloned into the plasmid vector, p3xFLAG-Myc-CMV<sup>TM</sup>-23,  
295 in which the gene expression is under the control of CMV promoter and expressed as a 3xFLAG-  
296 tagged protein. Initially, this panel of nsp1 $\beta$  mutants was analyzed in an IFN- $\beta$  promoter driven-  
297 luciferase reporter assay. The HEK-293T cells were co-transfected with a plasmid expressing  
298 wild type (WT) or mutated nsp1 $\beta$  and a reporter plasmid (p125-Luc) that expresses firefly  
299 luciferase reporter gene under the control of IFN- $\beta$  promoter. The empty vector (EV), p3xFLAG-  
300 Myc-CMV<sup>TM</sup>-23, was included in the analysis as a control. At 24 h post-transfection, cells were  
301 mock-infected or infected with Sendai virus (SeV). Cells were harvested to test the luciferase  
302 activities at 16 h post-infection (hpi). As shown in Figure 1A, SeV infection induced high level  
303 of luciferase reporter expression in cells transfected with empty vector, but luciferase expression  
304 was about 46 to 16-fold lower in cells expressing WT nsp1 $\beta$  and K124A mutant. In contrast, in  
305 comparison to that of WT nsp1 $\beta$ , about 33-fold, 19-fold, 24 fold and 26-fold higher level of  
306 reporter signal was detected in cells expressing R128A, R129A, RR129AA and 1 $\beta$ KO mutants,  
307 respectively. We further determined whether these mutations had effect on nsp1 $\beta$ 's ability to  
308 suppress IFN-dependent signaling pathway for the interferon-stimulated genes (ISGs)  
309 expression. The panel of nsp1 $\beta$  mutants was analyzed using an ISRE promoter driven-luciferase  
310 reporter assay. Similar result was generated as that obtained in Figure 1A, in comparison to that  
311 of cells expressing WT nsp1 $\beta$  about 38-fold, 46-fold, 75-fold and 71-fold higher level of reporter  
312 signal was detected in cells expressing R128A, R129A, RR129AA and 1 $\beta$ KO mutants,  
313 respectively (Figure 1B). These results suggest that R128 and R129 are critical to IFN antagonist

314 function of nsp1 $\beta$ . In contrast, K124 appeared to be not significantly affecting the IFN antagonist  
315 function of nsp1 $\beta$ .

316

317 The expression level of nsp1 $\beta$  was evaluated by western blot analysis using mAb M2 against  
318 FLAG-tag. The result confirmed the expression of nsp1 $\beta$  in WT and mutants-transfected cells  
319 used in luciferase assays (Figure 1C). In our previous study, we showed that double mutations of  
320 K124/R128 to A124/A128 caused increased amount of nsp1 $\beta$  expression in comparison to that of  
321 WT nsp1 $\beta$  and other mutants, which suggested that nsp1 $\beta$  may suppress its “self-expression”  
322 (26). In this study, individual substitutions introduced in K124, R128 and R129 showed that only  
323 R128A substitution affects the ability of nsp1 $\beta$  to suppress “self-expression” *in vitro*. The  
324 detailed mechanism for nsp1 $\beta$ 's ability to suppress “self-expression” and whether such property  
325 relates to innate immune suppression function of the virus needs to be further studied (see more  
326 details in Discussion section).

327

328 We further determined whether mutations introduced in GKYLQRRLQ motif also affect the  
329 transactivator function of nsp1 $\beta$ . A vaccinia/T7 polymerase system expressing nsp1 $\beta$ -2 region  
330 was used to analyze the expression of nsp2 and PRF products. The expression of -2 PRF product  
331 (nsp2TF) was determined by immunoprecipitation (IP) and Western blot (WB). Equal amount of  
332 lysates of transfected cells expressing WT nsp1 $\beta$ -2 or its mutants (K124A, R128A, R129A,  
333 1 $\beta$ KO, and RR129AA) were subjected to immunoprecipitation using the polyclonal Ab (pAb-  
334 TF) that specifically recognizes the C-terminal peptide of nsp2TF. Subsequently, western blot  
335 analysis was performed using pAb-TF and mAb140-68 that recognizes the N-terminal PLP2  
336 domain of the protein. As shown in Figure 2A, the nsp2TF product only detected in cells

337 expressing nsp1 $\beta$ -2 WT or K124A mutant, but not detected in cells expressing R128A, R129A,  
338 RR129AA mutants. In contrast, the expression of full-length nsp2 and nsp1 $\beta$  was detected in WT  
339 and all mutants of nsp1 $\beta$ -2 (Figure 2B). The result indicates that residue R128 and R129 are  
340 critical for the transactivator function of nsp1 $\beta$  in activating -2 PRF. K124 did not show  
341 significant effect on the nsp1 $\beta$  function in PRF transactivation.

342

### 343 ***In vitro* characterization of recombinant viruses containing mutations in GKYLQRRLQ** 344 **motif**

345 To further investigate whether the specific substitutions introduced into the nsp1 $\beta$   
346 GKYLQRRLQ motif of the virus could improve innate immune responses in PRRSV-infected  
347 cells, we created a panel of recombinant viruses using reverse genetics. Three viable  
348 recombinant viruses were generated, including vSD95-21-R128A (vR128A), vSD95-21-R129A  
349 (vR129A) and vSD95-21-R128A/R129A (vRR129AA), carrying single or double mutations at  
350 the residue R128 and R129 of the GKYLQRRLQ motif. As a comparison, recombinant viruses  
351 with the mutation at K124 (vSD95-21-K124A; vK124A), the double mutations at K124/R128  
352 (vSD95-21-K124A/R128A; v1 $\beta$ KO), and the WT virus, vSD95-21 were also recovered from  
353 reverse genetics. Stability of those mutations introduced into the virus was determined by serially  
354 passaging each virus 5 times in MARC-145 cells, and sequence analysis of passage 3 and  
355 passage 5 viruses showed that all of the introduced mutations were stably maintained in the  
356 mutant viruses. The growth property of these mutants (passage 3) was compared with the WT  
357 parental virus. In comparison to WT virus (peak viral titer of  $10^{7.33}$  TCID<sub>50</sub>/ml), vK124A showed  
358 similar growth ability, while vR128A and vR129A showed certain levels of reduced growth  
359 ability (peak viral titers of  $10^{7.0}$  TCID<sub>50</sub>/ml and  $10^{6.58}$  TCID<sub>50</sub>/ml, respectively). In contrast,



360 vRR129AA and v1 $\beta$ KO mutants had significantly reduced growth ability with about 1~1.5 logs  
361 decrease in viral titer through the time course of study (Figure 3A). Plaque assay result  
362 consistently showed that v1 $\beta$ KO and vRR129AA developed smaller plaques than that of WT  
363 virus (Figure 3B).

364

### 365 **Expression of innate immune genes in nsp1 $\beta$ mutant virus-infected cells**

366 As we determined that R128A and/or R129A mutations introduced in GKYLQRRLQ motif  
367 reduced the nsp1 $\beta$ 's ability to suppress innate immune response (Figure 1), we further analyzed  
368 whether these mutations could alter the inhibitory effect of PRRSV on type I IFN production and  
369 signaling. Since K124A did not show much effect on the function of nsp1 $\beta$  in PRF  
370 transactivation and innate immune suppression, recombinant viruses containing K124A  
371 substitution (vK124A and v1 $\beta$ KO) were not further analyzed in the following experiments (see  
372 Discussion section for more description about the characteristics of v1 $\beta$ KO). Initially, IFN- $\alpha$   
373 expression was evaluated in nsp1 $\beta$  mutants or WT virus-infected porcine alveolar macrophages  
374 (PAMs) using ProcartaPlex Porcine IFN alpha Simplex kit (eBioscience, San Diego, CA). PAMs  
375 were initially infected with equal amount (MOI=1) of WT or an nsp1 $\beta$  mutant. At 12 h post-  
376 infection, IFN- $\alpha$  concentration in the cell culture supernatant of virus-infected porcine alveolar  
377 macrophages (PAM) was evaluated. All of the nsp1 $\beta$  mutants showed improved ability to induce  
378 the production of IFN- $\alpha$ , which is indicated by 3.3-fold (vR128A), 6.1-fold (vR129A), and 50-  
379 fold (vRR129AA) higher concentration of IFN- $\alpha$  in the supernatant of mutant viruses infected  
380 cells than that of WT virus infected cells (Figure 4A). Of note, vRR129AA showed the strongest  
381 stimulation of IFN- $\alpha$  production. In addition, the expression of nsp1 $\beta$  was detected by western  
382 blot, indicating successful viral replication in PAM of WT virus and nsp1 $\beta$  mutants (Figure 4E).

383 Subsequently, we analyzed whether these mutations could alter the inhibitory effect of PRRSV  
384 on the production of ISGs. At 12 h post-infection, the mRNA expression level of three selected  
385 ISGs, ISG15, IFIT1 and IFITM1, was assessed via quantitative real-time PCR using predesigned  
386 primers/probe sets (Applied Biosystems, Foster city, CA). Consistent with their improved ability  
387 for IFN- $\alpha$  induction, all of the nsp1 $\beta$  mutants stimulated higher mRNA expression level of ISGs.  
388 As indicated in Figure 4B, in comparison with that of WT virus infected cells, about 4.1-fold  
389 (vR128A), 7.8-fold (vR129A) and 20-fold (vRR129AA) higher mRNA expression of ISG15 was  
390 detected in mutant viruses infected cells, although the increase in vR128A and vR129A infected  
391 cells is not statistically significant. Similarly, the mRNA expression levels of IFIT1 and IFITM1  
392 were increased in mutant viruses infected cells in comparison to that in WT virus infected cells  
393 (Figure 4C and 4D).

394

#### 395 ***In vivo* characterization of nsp1 $\beta$ mutants**

396 Subsequently, we obtained five groups of 4-week-old pigs to determine whether the R128 and  
397 R129-related mutants could improve specific immune responses in PRRSV-infected pigs. As  
398 shown in Table 1, each group of pigs (n=9) was infected with the WT virus, an nsp1 $\beta$  mutant, or  
399 mock-infected with cell culture medium as negative control. The serum, BALF, and lung lysate  
400 samples were collected and stored at -80 °C for further analysis. We did not observe any  
401 noticeable clinical PRRS symptoms and fever in any of the WT virus or nsp1 $\beta$  mutant-infected  
402 pigs.

403

404 ***Viral load in serum and tissue samples.*** Initially, we measured viral RNA load in serum samples  
405 using real-time quantitative RT-PCR (qRT-PCR). In comparison with the group of pigs infected

406 with WT virus, pigs infected with vR128A and vRR129AA mutants showed consistently lower  
407 viral RNA load through the entire time course of the experiment, while pigs infected with  
408 vR129A mutant exhibited lower viral RNA load from 1 DPI to 14 DPI (Figure 5A). In pigs  
409 infected with the vR128A mutant, statistically significant lower level of viral RNA load was  
410 obtained at 1, 2, 5, and 14 DPI, in comparison to that in pigs infected with WT virus (Figure 5A).  
411 At most of the time-points, especially at the later stage of the infection, the mean viral RNA load  
412 in pigs infected with vRR129AA mutant was the lowest among all the infected pigs (Figure 5A).  
413 Surprisingly, vR129A mutant infected pigs showed similar level of mean viral RNA load as the  
414 group of pigs infected with WT virus at 21 DPI, and exhibited higher (but not statistically  
415 significant) viral RNA load than that of pigs infected with WT virus at 28 DPI and 35 DPI.

416 Since qRT-PCR does not distinguish between viable and nonviable forms of the virus, we further  
417 quantified infectious virus particles in serum samples. Infectious virus titer was measured  
418 through micro-titration assay using MARC-145 cells. At 1, 2 and 5 DPI, infectious viral titers in  
419 groups of pigs infected with nsp1 $\beta$  mutants were about 1~3 log lower (statistically significant)  
420 than the viral titers in pigs infected with WT virus (Figure 5B), which is consistent with viral  
421 loads quantified by qRT-PCR (Figure 5A). The infectious viral titer in many pigs infected with  
422 nsp1 $\beta$  mutants was lower than the detection limit ( $10^{1.67}$  TCID<sub>50</sub>/ml) of the micro-titration assay  
423 through the time course of infection. The rebounded viral titer was observed in vR129A mutant-  
424 infected pigs at 21, 28 and 35 DPI, which is consistent with the viral RNA load data generated by  
425 qRT-PCR. These results indicate that the growth ability of vR128A and vRR129AA was  
426 attenuated *in vivo*, and the growth ability of vR129A was attenuated at early stage of infection  
427 but reverted to WT phenotype at certain level during the later stage of infection (see sequencing  
428 data in Table 2).

429 Since PAM serves as the primary target cell for PRRSV, we further evaluated the viral load in  
430 lung lysate and BALF collected at 7, 21 and 35 DPI. Viral RNA load was quantified by qRT-  
431 PCR and infectious viral titer was determined by micro-titration assay. Results from both qRT-  
432 PCR and micro-titration assay showed that the viral loads in lung and BALF from all groups of  
433 pigs infected with *nsp1β* mutants were consistently lower than that in pigs infected with WT  
434 virus at 7 and 21 DPI (Figure 6), although some of the differences were not statistically  
435 significant. At 35 DPI, the lower level of mean viral load and infectious viral titer were detected  
436 in lung samples from pigs infected with vR128A and vRR129AA mutants, in comparison with  
437 that in pigs infected with WT virus (Figure 6). In the lung samples from vR129A mutant infected  
438 pigs, the mean viral load and infectious viral titer were reached similar level as that of WT virus-  
439 infected pigs at 35 DPI. These results suggest that *nsp1β* mutants have attenuated replication  
440 ability in the lung of infected pigs, but vR129A showed reversion to WT phenotype at certain  
441 level during later stage of infection.

442 ***Genetic stability of nsp1β mutants in pigs.*** The genetic stability is one of the important criteria  
443 for selecting vaccine candidates. Initially, serum samples from 3 pigs per group terminated at 21  
444 DPI were used to determine the stability of the introduced mutations. The *nsp1β* coding region  
445 was RT-PCR amplified and the PCR product was subjected to DNA sequencing analysis. As  
446 showed in Table 2, no 2<sup>nd</sup> site mutation and also no reversion were found in *nsp1β* coding region  
447 of the virus that isolated from serum samples of the pigs infected by vRR129AA mutant virus. In  
448 the group of pigs infected with vR128A mutant, the designed mutation was maintained in the  
449 viruses recovered from all three tested pigs, but several 2<sup>nd</sup> site mutations were observed,  
450 including the substitution of Asp<sup>9</sup> to Gly and Ser<sup>122</sup> to Pro in all three pigs, and His<sup>109</sup> and Leu<sup>141</sup>  
451 substituted by Arg and Pro in one pig, respectively. In the group of pigs infected with vR129A

452 mutant, the designed mutation in one of the three tested pigs reversed from Ala back to Arg (in  
453 WT virus), and R129A was maintained in the other two pigs. Similar to vR128A group, 2<sup>nd</sup> site  
454 mutation, Ser<sup>122</sup> to Pro, was detected in those two pigs that maintained designed mutation; an  
455 additional mutation of Ser<sup>169</sup> to Pro occurred in one of the two pigs, and the substitution of Asp<sup>9</sup>  
456 to Gly was observed in all three pigs. Since there was a reversion occurred in one of the vR129A  
457 mutant-infected pig at 21 DPI, we further analyzed serum samples from all 6 pigs infected with  
458 vR129A at 14 DPI. Remarkably, the pig with Ala<sup>129</sup> to Arg reversion at 21 DPI had already  
459 obtained the reversion at 14 DPI. However, the designed R129A mutation was maintained in all  
460 other five pigs. It is worth noting that the 2<sup>nd</sup> site substitution of Ser<sup>122</sup> to Pro occurred in all of  
461 the pigs that maintained designed mutations (R128A and R129A) at 14, 21 and 35 DPI,  
462 suggesting that this substitution may compromise the effect of designed mutations on viral  
463 growth ability *in vivo*. Interestingly, the mutation of Asp<sup>9</sup> to Gly was not only detected in pigs  
464 infected with all mutants, but also observed in pigs infected with WT virus. This mutation may  
465 relate to the *in vivo* fitness of PRRSV, which was most likely not caused by our designed  
466 mutations. In addition, using the serum samples at 35 DPI that was determined to be PRRSV  
467 RNA positive by real-time RT-PCR, no reversion was observed in sequencing analysis. We  
468 searched PRRSV full-length genome sequences available in the Genbank (as of 7/27/2015), all  
469 of the 2<sup>nd</sup> site substitutions that observed here are able to be found in field strains, for example,  
470 PRRSV P129 strain contains Pro<sup>122</sup>. Taken together, among the three nsp1 $\beta$  mutants, vRR129AA  
471 maintained the best genetic stability *in vivo* with no reversion and less 2<sup>nd</sup> site mutation detected  
472 in nsp1 $\beta$ -coding region.

473 ***Innate immune response in PRRSV nsp1 $\beta$  mutants infected pigs.*** To determine whether the  
474 mutations introduced into nsp1 $\beta$  region could improve PRRSV-specific innate immune response,

475 we initially measured IFN- $\alpha$  expression in infected and control pigs during the early stage of  
476 infection. Compared to WT virus-infected pigs, a 1.5-fold higher (but was not significant) levels  
477 of IFN- $\alpha$  was observed in serum samples of vRR129AA infected pigs at 1 DPI (data not shown).  
478 Since the virus replicates primarily in alveolar macrophages and we inoculated the virus by  
479 intranasal (IN) route, the immune response in the lung is important, we measured IFN- $\alpha$  levels in  
480 both BALF (represents airways) and lung lysate (represents lung parenchyma, local site of  
481 PRRSV infection). In the BALF at 7 DPI, the IFN- $\alpha$  was comparable among all pig groups,  
482 while at 21 and 35 DPI in pigs inoculated with vRR129AA and vR129A mutant viruses, there  
483 was an increased level (but not statistically significant) of IFN- $\alpha$  production compared to that of  
484 WT virus-infected pigs (data not shown). At 7 DPI, in the lung lysate of pigs inoculated with  
485 nsp1 $\beta$  mutant viruses, higher levels of IFN- $\alpha$  were observed compared to that of WT virus-  
486 infected pigs (Figure 7A).

487 IFN- $\alpha$  is critical for natural killer (NK) cell-mediated cytotoxic function. To determine whether  
488 the nsp1 $\beta$  mutations impaired IFN- $\alpha$  antagonist function of the virus, PBMCs from mutants and  
489 WT virus-infected pigs were used as a source of NK cells to evaluate NK cell function in the NK  
490 cell-cytotoxicity assay. At both the E:T ratios (100:1 and 50:1), the vRR129AA mutant virus-  
491 infected pigs had increased activity of NK cell cytotoxic function at 7 DPI (Figure 7B and C).  
492 This result is consistent with the increased level of IFN- $\alpha$  production in the serum and lung  
493 lysate of vRR129AA-infected pigs.

494 ***Adaptive immune response in PRRSV nsp1 $\beta$  mutants infected pigs.*** A strong innate immune  
495 response following a virus infection augments the cell-mediated adaptive immunity. Therefore,  
496 we analyzed the production of an important Th1 cytokine IFN- $\gamma$  response in WT virus and nsp1 $\beta$

497 mutants-infected pigs. The production of IFN- $\gamma$  in the serum of WT virus-infected pigs was  
498 undetectable throughout the time course of the study (0-35 DPI), while in the serum of nsp1 $\beta$   
499 mutants-infected pigs, spurts of IFN- $\gamma$  secretion (100-150 pg/ml) was detected at multiple DPIs,  
500 with IFN- $\gamma$  detected from vR129A mutant-infected pigs at 7-21 DPI, and IFN- $\gamma$  detected from  
501 vRR129AA mutant infected pigs at 14 and 28 DPI (Figure 8A). In vR128A mutant-infected pigs,  
502 increased IFN- $\gamma$  in serum was detected at 5 and 14 DPI (Figure 8A). Such an early response of  
503 IFN- $\gamma$  in nsp1 $\beta$  mutants-infected pigs might be due to the rescue of adaptive immunity mediated  
504 through induction of IFN- $\alpha$  secretion and NK cell function by these mutants. A similar increase  
505 in IFN- $\gamma$  secretion (but not statistically significant) was detected in the BALF of vR128A,  
506 vR129A and vRR129AA infected pigs, observed at only 7 DPI (data not shown). However, an  
507 increased level of IFN- $\gamma$  production in the lung lysate of vR129A and vRR129AA infected pigs  
508 at 7 DPI was significantly higher than that of WT virus-infected pigs (Figure 8B).

509 Production of the pro-inflammatory cytokine IL-6 suggests the inflammatory reaction in the  
510 lungs of pigs (34). The levels of IL-6 was higher (but not significant) at 21 DPI in the BALF of  
511 vR129A and vRR129AA infected pigs compared to that of WT virus infected pigs (Figure 8C).  
512 In the lung lysate of vRR129AA infected pig at 21 DPI, a significantly higher level of IL-6  
513 production was detected compared to that of WT virus infected pigs (Figure 8D). This data  
514 suggests that the induction of IL-6 production by the vRR129AA mutant virus in pigs appears to  
515 be responsible for augmenting the IFN- $\gamma$  production, an indicator of adaptive immunity.

516 We further evaluated the frequency of different T cell subpopulation in PBMCs, expressed as the  
517 percentage of CD3<sup>+</sup> or CD3<sup>-</sup> cells. The pig T cells expressing the combination of phenotypic  
518 markers CD3<sup>+</sup>CD4<sup>-</sup>CD8 $\alpha$ <sup>+</sup> are either cytotoxic T cells (CTLs) or  $\gamma\delta$  T cells, and cells with

519 CD3<sup>+</sup>CD4<sup>-</sup>CD8αβ<sup>+</sup> are exclusively CTLs (38, 39). Porcine immune system has a unique  
520 frequency of CD3<sup>+</sup>CD4<sup>+</sup>CD8α<sup>+</sup> T cells, which have the memory, cytotoxic, and T-helper cell  
521 properties (40, 41). To determine antigen specific activation of T cell response, IFN-γ secreting  
522 lymphocyte subsets were elucidated by re-stimulating PBMCs with the same virus *in vitro*. In  
523 every phenotypic marker staining, respective isotype controls were included to eliminate the  
524 background. The specific population of cells was identified based on combination of phenotypic  
525 cell surface markers, which include CD3<sup>+</sup>CD4<sup>-</sup>CD8α<sup>+</sup> (CTLs or γδ T cells), CD3<sup>+</sup>CD4<sup>+</sup>CD8α<sup>+</sup>  
526 (T-helper/memory), and CD3<sup>-</sup>CD4<sup>-</sup>CD8α<sup>+</sup> (NK) cells (38, 40-43). Subsequently, the cells were  
527 fixed and stained for intracellular IFN-γ and gated for their respective activated (IFN-γ<sup>+</sup>)  
528 phenotype. Frequency of total CTLs/γδ T cells in vR129A and vRR129AA infected pigs were  
529 numerically increased (but not statistically significant) at 21 DPI and were significantly reduced  
530 at 35 DPI compared to WT virus infected pigs (Figure 9A), while the activated (IFN-γ<sup>+</sup>)  
531 CTLs/γδ T cells in the same mutants infected pigs were numerically increased and decreased  
532 (but not statistically significant) compared to WT virus at DPI 7 and 35, respectively (Figure  
533 9B). In comparison of WT virus-infected pigs with vR129A and vRR129AA-infected pigs,  
534 exactly a similar trend (but not statistically significant) in total and activated T-helper/memory  
535 cell frequencies to that of CTLs/γδ T cells was observed at all three DPIs (Figure 9C and D). The  
536 frequency of NK cells was significantly increased only in vRR129AA infected pigs at 7 DPI  
537 (Figure 9E). This data suggest that the NK cells and the two important T cell subsets were  
538 activated particularly in vRR129AA mutant PRRSV-infected pigs, suggesting the virus specific  
539 activation of innate and adaptive immunity.

540

541



542 **DISCUSSION**

543 Many studies have demonstrated that a potent innate immune response induced by microbial  
544 infection / vaccination will lead to generation of sufficient adaptive immunity, which  
545 subsequently clears the pathogen infection from the host completely (44, 45). However, PRRSV  
546 infection generally induces poor anti-viral innate IFN and cytokine responses, which results in  
547 weak adaptive immunity (46-50). One of the key steps in new PRRS vaccine construction is to  
548 develop strategies to target these initial immune response events to enhance the viral specific  
549 immunity. Previous studies for other viral pathogens showed that recombinant viruses generated  
550 with targeted mutations (deletions) in genes encoding for immune antagonists are excellent  
551 candidates for MLV vaccines (51-54). The (selected) recombinant viruses normally grow well in  
552 tissue culture; while in infected animals, they are attenuated but still replicate to sufficient  
553 amounts for stimulating robust immune responses. Several PRRSV proteins have been identified  
554 as antagonists to the type I IFN induction (and signaling), and nsp1 $\beta$  was determined having the  
555 strongest inhibitory effect among those proteins (22-24, 26). Therefore, in this study, our vaccine  
556 development strategy is to generate recombinant viruses with targeted mutations in the nsp1 $\beta$   
557 regions.

558 Our previous study identified a highly conserved GKYLQRRLQ motif in nsp1 $\beta$  that is critical  
559 for its inhibitory effect on type I IFN production and signaling. Based on the crystal structure of  
560 nsp1 $\beta$ , three basic residues (K124, R128, and R129) in GKYLQRRLQ motif are exposed on the  
561 surface of the protein. In our previous study, double mutations of K124A/R128A impaired the  
562 IFN antagonist function of nsp1 $\beta$  (26). In this study, we further tested each of these three  
563 individual residues. In comparison to WT nsp1 $\beta$ , nsp1 $\beta$  mutants carrying alanine substitution at  
564 R128 and R129 showed a significantly reduced antagonism effect on reporter gene expression

565 under the control of IFN- $\beta$  promoter (p125-Luc); however, K124A mutant still had a similar  
566 inhibitory effect on reporter gene expression as that of WT nsp1 $\beta$ . Similar results were observed  
567 in the luciferase reporter assay (pISRE-Luc) utilized to examine the inhibitory effect on type 1  
568 IFN signaling. Both the WT nsp1 $\beta$  and K124A mutant severely suppressed luciferase reporter  
569 expression, in contrast to significant higher level of luciferase expression in cells transfected with  
570 nsp1 $\beta$  mutants that contain mutations at R128 and/or R129 (Figure 1B). These results indicate  
571 that R128 and R129 residues, but not K124, are critical for nsp1 $\beta$ 's function in antagonizing type  
572 1 IFN production and signaling.

573 As we discussed previously (26), suppressing host cellular gene expression, including nsp1 $\beta$   
574 "self-expression" could be a mechanism of its immune antagonist function. Compared to the  
575 expression level of WT nsp1 $\beta$ , obviously higher level of nsp1 $\beta$  expression was detected in  
576 western blot analysis for R128A and K124A/R128A (1 $\beta$ KO) mutants (Figure 1C). Interestingly,  
577 when R129A substitution combines with R128A (RR129AA), it appeared to restore the nsp1 $\beta$ 's  
578 ability to suppress its "self-expression". The single alanine substitution of R129 residue did not  
579 impair the ability of nsp1 $\beta$  to suppress its "self-expression", although it attenuated nsp1 $\beta$ 's  
580 ability to suppress type I IFN expression. These data make us speculate that different  
581 mechanisms may be utilized by R128 and R129 residues to evade host innate immune defense,  
582 which needs to be further elucidated.

583 As we discussed above, besides function as an innate immune antagonist, nsp1 $\beta$  was recently  
584 identified as a transactivator for the expression of -2/-1 PRF products, nsp2TF and nsp2N. Both  
585 nsp2TF and nsp2N share the N-terminal 2/3 sequence with nsp2, which contains the PLP2  
586 domain. PLP2 was also identified as an innate immune antagonist that is capable of removing  
587 ubiquitin (Ub) and Ub-like modifiers like ISG15 from host cell substrates (55-58). When testing

588 the nsp1 $\beta$  effect during viral infection (see below), it remains to be established to what extent  
589 nsp1 $\beta$  directly modulates the innate immune response or does so by stimulating the expression of  
590 nsp2TF and nsp2N.

591 In this study, we generated recombinant viruses of nsp1 $\beta$  mutants using reverse genetics,  
592 including vK124A, vR128A, vR129A and vRR129AA. As a comparison, our previously  
593 constructed mutant v1 $\beta$ KO (containing double mutations of K124A/R128A) was included in  
594 viral growth characterization in cell culture. In comparison to WT virus, all nsp1 $\beta$  mutants  
595 except vK124A had attenuated growth ability in cell culture, but their peak viral titers were all  
596 reached above 5 logs TCID<sub>50</sub>/mL, which is acceptable for subsequently application in animals.  
597 Multiple-step viral growth curves showed that vR128A and vR129A had slightly slower growth  
598 kinetics, while v1 $\beta$ KO and vRR129AA showed 1~1.5 logs lower virus titer than that of parental  
599 virus at all the tested time points (Figure 3A). It is worth noting that v1 $\beta$ KO containing the  
600 double mutations of K124A/R128A had lower virus titer than that of mutant virus with single  
601 mutation of R128A, but single K124A mutation did not affect much on the virus growth ability  
602 in cell culture. In addition, none of the mutations affected the release of nsp1 $\beta$  from nsp1 $\beta$ -2  
603 polyprotein (Figure 2B), suggesting that the reduced growth rate (viral titer) of the nsp1 $\beta$   
604 mutants may not directly caused by a basic defect in replicase polyprotein proteolysis. We  
605 speculate that R128A, R129A, or combined K124A/R128A, and R128A/R129A mutations may  
606 change nsp1 $\beta$  protein or RNA structure, which in turn affects virus replication ability. The in  
607 depth mechanism of these mutations that affects viral growth ability requires more studies in the  
608 future. When tested in the vaccinia/T7 expression system, the expression of nsp2TF was  
609 impaired by alanine substitutions at residue 128 and 129 using nsp1 $\beta$ -2 expression constructs  
610 (Figure 2A). Under the virus infection condition, these two residues are also essential for the

611 PRF transactivator function of nsp1 $\beta$  (data not shown). Taken together, our data indicate that the  
612 three basic amino acids exposed on nsp1 $\beta$  surface appear to have different functions, and the  
613 detailed mechanism needs to be further elucidated.

614 Subsequently, these mutants were characterized in nursery pigs. Since the K124A did not have  
615 much effect on innate suppression function of nsp1 $\beta$ , and the recombinant virus containing  
616 K124A mutation did not affect much on viral replication, this mutant was excluded in current  
617 animal study. In a previous study, we evaluated 1 $\beta$ KO and WT viruses in pigs. The 1 $\beta$ KO  
618 showed over-attenuated phenotype with virus grew in extremely low titer ( $\sim 5 \times 10^4$  RNA  
619 copies/ml in serum), which is 2 to 3 logs lower than that of wild type virus. As a consequence,  
620 pigs did not seroconvert until 28 dpi. The initial IFN- $\alpha$  response was very limited (8.4 pg/mL  
621 serum at 3 DPI); in contrast, we could detect certain level of IFN- $\alpha$  response (100.9 pg/mL  
622 serum at 3 DPI) in WT virus-infected pigs. As we discussed above, single mutation on K124  
623 residue did not seem to affect much on the *in vitro* growth ability of the virus, but combined  
624 mutations with R128 significantly impaired the virus growth ability *in vitro* and *in vivo*. The in  
625 depth mechanism of K124 involved in viral replication and its function in relation to combined  
626 effect of R128 mutation need to be further studied. Since our previous data showed over-  
627 attenuated phenotype of 1 $\beta$ KO, in the current study, we focused on characterizing the other three  
628 nsp1 $\beta$  mutants (vR128A, vR129A, and vRR129AA) in nursery pigs. Active virus replication was  
629 observed in all of the virus-infected pigs. The viremia data indicate that, in consistent with *in*  
630 *vitro* results, nsp1 $\beta$  mutants were also attenuated in pigs. At all the time-points, in comparison to  
631 WT virus-infected pigs, vR128A- and vRR129AA-infected pigs had consistently lower levels of  
632 mean viral RNA load and infectious virus titer. For vR129A group, these pigs also had lower  
633 levels of viremia than that of WT virus group at the early time-points; however, they showed

634 even higher level of viremia than that of WT group at 35 DPI. These results suggest that the  
635 virus in vR129A could be reversed back to WT virus. Subsequently, sequence analysis of nsp1 $\beta$   
636 coding region was performed to confirm the stability of the mutations introduced into the virus.  
637 From viruses recovered at 21 DPI, the designed alanine substitutions were stably maintained,  
638 except a reversion identified in one of the pigs (pig #31) infected with vR129A. We further  
639 sequenced nsp1 $\beta$  coding region in the viruses recovered from vR129A infected pigs at 14 DPI,  
640 the result showed that the reversion only occurred in pig #31, but not the other five tested pigs.  
641 Unexpectedly, no reversion in the nsp1 $\beta$  coding region was identified in vR129A group of pigs  
642 at 35 DPI, although vR129A group of pigs showed even higher virus titer than that of WT group  
643 of pigs. We speculate that the spontaneous mutations in other regions of viral genome may  
644 compensate viral replication ability *in vivo*. Remarkably, for those viruses stably maintained the  
645 designed mutations vR128A and vR129A in infected pigs, a specific 2<sup>nd</sup> site mutation of Ser<sup>122</sup> to  
646 Pro<sup>122</sup> was consistently identified. We analyzed the sequence of nsp1 $\beta$  from *in vitro* expression  
647 plasmids and original recombinant viruses that grew in MARC-145 cells (before inoculation into  
648 pigs), and the result showed that Ser<sup>122</sup> was stably maintained in vR128A, vR129A and  
649 vRR129AA. The data suggest that Pro<sup>122</sup> may contribute the viral fitness *in vivo* and Ser<sup>122</sup> to  
650 Pro<sup>122</sup> substitution may compromise the side effect of our designed mutations on virus  
651 replication ability in animals. Whether the Ser<sup>122</sup> to Pro<sup>122</sup> substitution has effect on the function  
652 of nsp1 $\beta$  needs to be further studied.

653 Given the impaired ability of nsp1 $\beta$  mutants vR128A, vR129A and vRR129AA to antagonize  
654 innate immune response *in vitro*, we further assessed the ability of these viruses in the induction  
655 of host immune response *in vivo*. After immunization, no clinical symptoms and adverse side  
656 effects were observed in the WT and mutant virus-infected pigs. In addition, when terminated

657 three pigs per group at 7, 21 and 35 DPI, no obvious lung lesion was observed. This result is  
658 expected, since the WT virus SD95-21 (backbone of nsp1 $\beta$  mutants) has 99.5% nucleotide  
659 identity with that of VR2332, the parental virus of PRRS modified live virus (MLV) vaccine  
660 (Ingelvac PRRS MLV; Boehringer Ingelheim Vetmedica, Inc.), and 99.6% identity to Ingelvac  
661 PRRS MLV. In addition, SD 95-21 virus was adapted growth in MARC-145 cells. In previous  
662 studies, pigs infected with PRRS MLV strain of VR2332 showed very mild or undetectable  
663 clinical, gross and histopathological lesions (59). The goal of our vaccine development is to  
664 improve the ability of current MLV vaccine to stimulate higher innate and cell mediated immune  
665 responses.

666 Since type 1 IFNs are the principle cytokines for innate immunity against viral infections, IFN- $\alpha$   
667 was selected as a representative to assess the ability of PRRSV to induce host innate immune  
668 response. In consistent with our data generated in *in vitro* expression system, nsp1 $\beta$  mutants  
669 induced higher level of IFN- $\alpha$  than that of WT virus during early time period post-infection. In  
670 comparison to that of WT virus infected pigs, higher cytotoxic activity of NK cells was also  
671 observed in pigs infected with nsp1 $\beta$  mutants. These results suggest that PRRSV nsp1 $\beta$  plays a  
672 crucial role in suppressing host innate immunity, and modifying this protein could effectively  
673 improve the ability of PRRSV to stimulate host innate immune response. Furthermore, these  
674 mutants induced earlier and higher level of IFN- $\gamma$  expression compared to WT virus. As an  
675 important factor in adaptive immunity against viral infection, IFN- $\gamma$  increases antigen  
676 presentation and promotes Th1 cell differentiation (60). The increased expression of IFN- $\gamma$  in  
677 mutant viruses infected pigs indirectly indicates the activation of Th1 cell-mediated immune  
678 response. This was observed not only in serum of mutants infected pigs, but also indicated by  
679 increased activation of CTLs/ $\gamma\delta$  T, T-helper/memory, and NK cells. Previously, increased

680 frequency of activated T-helper/memory cells in pigs was shown to be beneficial in virus  
681 clearance in Aujeszky's disease virus, African and Classical swine fever virus, and PRRSV  
682 infections (33, 41, 61-64). Taken together, besides induction of higher level innate immune  
683 response, these mutants may also have stronger ability in augmenting Th1 cell-mediated  
684 adaptive immunity in comparison to that of WT virus. As a candidate vaccine, one would expect  
685 its ability to stimulate significant humoral response in animals. In fact, we performed both  
686 neutralizing antibody and ELISA assays using serum samples, but the result showed no  
687 significant difference among pig groups infected with WT virus and three nsp1 $\beta$  mutants (data  
688 not shown). It is a well-established phenomenon that strong Th1 response suppresses the Th2  
689 response (humoral response) and vice-versa, which were demonstrated previously in mice (65,  
690 66) and pigs (33, 64, 67). Therefore, our data suggest that lack of improved virus neutralizing  
691 antibody response in nsp1 $\beta$  mutants-infected pigs could be caused by the strong Th1 response.  
692 Future virus challenge study in the nsp1 $\beta$  mutant vaccinated pigs may reveal benefits of  
693 increased Th1 response in viral clearance.

694 Based on our data, the nsp1 $\beta$  mutant, vRR129AA, could be a potential vaccine candidate, and  
695 this attenuation strategy could be easily applied to improve current vaccines. This conclusion is  
696 based on multiple observations. First, vRR129AA can grow to sufficient virus titers in cell  
697 culture (greater than 5 log TCID<sub>50</sub>/mL), which facilitate large scale vaccine production. Second,  
698 in comparison to WT virus, vRR129AA induced earlier and stronger innate immune response,  
699 which was supported by elevated IFN- $\alpha$  expression and NK cell cytotoxic activity. The improved  
700 innate immune response appears to augment cell-mediated adaptive immunity, indicated by early  
701 induction of IFN- $\gamma$  expression by both NK cells and T cells, followed by depletion of activated T  
702 cell subsets as presented in phenotypic analysis of PBMCs. Another important aspect is that this

703 mutant appeared to be quickly cleared from virus-infected pigs, and showed better genetic  
704 stability than nsp1 $\beta$  mutants containing single alanine substitution (vR128A, vR129A).  
705 Nevertheless, the protection efficacy of this potential vaccine candidate needs to be further  
706 assessed in animal challenge study. Finally, R128 and R129 residues are highly conserved in all  
707 available PRRSV strains as described previously (25, 26), in which the technology described in  
708 this study can be easily applied to current commercial vaccines and other candidate vaccines.

709

#### 710 **ACKNOWLEDGEMENTS**

711 We thank Professor Eric J. Snijder (Leiden University Medical Center, Leiden, The Netherlands)  
712 for helpful discussion, Russell Ransburgh and Elizabeth Poulsen (Kansas State University,  
713 Manhattan, KS, USA) for technical assistance. This project was supported by Agriculture and  
714 Food Research Initiative Competitive Grant no. 2012-67015-21823 from the USDA National  
715 Institute of Food and Agriculture; Kansas State University research startup fund.



## 716 REFERENCES

- 717 1. **Keffaber KK.** 1989. Reproductive failure of unknown etiology. *Am. Assoc. SwinePract.*  
718 *Newsl.*:1-9.
- 719 2. **Wensvoort G, Terpstra C, Pol JM, ter Laak EA, Bloemraad M, de Kluyver EP,**  
720 **Kragten C, van Buiten L, den Besten A, Wagenaar F, et al.** 1991. Mystery swine  
721 disease in The Netherlands: the isolation of Lelystad virus. *Vet Q* **13**:121-130.
- 722 3. **Benfield DA, Nelson E, Collins JE, Harris L, Goyal SM, Robison D, Christianson**  
723 **WT, Morrison RB, Gorcyca D, Chladek D.** 1992. Characterization of swine infertility  
724 and respiratory syndrome (SIRS) virus (isolate ATCC VR-2332). *J Vet Diagn Invest*  
725 **4**:127-133.
- 726 4. **Collins JE, Benfield DA, Christianson WT, Harris L, Hennings JC, Shaw DP, Goyal**  
727 **SM, McCullough S, Morrison RB, Joo HS, et al.** 1992. Isolation of swine infertility  
728 and respiratory syndrome virus (isolate ATCC VR-2332) in North America and  
729 experimental reproduction of the disease in gnotobiotic pigs. *J Vet Diagn Invest* **4**:117-  
730 126.
- 731 5. **Albina E, Madec F, Cariolet R, Torrison J.** 1994. Immune response and persistence of  
732 the porcine reproductive and respiratory syndrome virus in infected pigs and farm units.  
733 *Vet Rec* **134**:567-573.
- 734 6. **Dwivedi V, Manickam C, Binjawadagi B, Linhares D, Murtaugh MP,**  
735 **Renukaradhya GJ.** 2012. Evaluation of immune responses to porcine reproductive and  
736 respiratory syndrome virus in pigs during early stage of infection under farm conditions.  
737 *Virology* **9**:45.
- 738 7. **Murtaugh MP, Xiao Z, Zuckermann F.** 2002. Immunological responses of swine to  
739 porcine reproductive and respiratory syndrome virus infection. *Viral Immunol* **15**:533-  
740 547.
- 741 8. **Renukaradhya GJ, Dwivedi V, Manickam C, Binjawadagi B, Benfield D.** 2012.  
742 Mucosal vaccines to prevent porcine reproductive and respiratory syndrome: a new  
743 perspective. *Anim Health Res Rev* **13**:21-37.
- 744 9. **Snijder EJ, Kikkert M, Fang Y.** 2013. Arterivirus molecular biology and pathogenesis.  
745 *J Gen Virol* **94**:2141-2163.
- 746 10. **Meulenberg JJ, Petersen-den Besten A, De Kluyver EP, Moormann RJ, Schaaper**  
747 **WM, Wensvoort G.** 1995. Characterization of proteins encoded by ORFs 2 to 7 of  
748 Lelystad virus. *Virology* **206**:155-163.
- 749 11. **Meulenberg JJ, Petersen-den Besten A, de Kluyver EP, Moormann RJ, Schaaper**  
750 **WM, Wensvoort G.** 1995. Characterization of structural proteins of Lelystad virus. *Adv*  
751 *Exp Med Biol* **380**:271-276.
- 752 12. **Mounir S, Mardassi H, Dea S.** 1995. Identification and characterization of the porcine  
753 reproductive and respiratory virus ORFs 7, 5 and 4 products. *Adv Exp Med Biol*  
754 **380**:317-320.
- 755 13. **Bautista EM, Meulenberg JJ, Choi CS, Molitor TW.** 1996. Structural polypeptides of  
756 the American (VR-2332) strain of porcine reproductive and respiratory syndrome virus.  
757 *Arch Virol* **141**:1357-1365.
- 758 14. **Mardassi H, Massie B, Dea S.** 1996. Intracellular synthesis, processing, and transport of  
759 proteins encoded by ORFs 5 to 7 of porcine reproductive and respiratory syndrome virus.  
760 *Virology* **221**:98-112.

- 761 15. **Meng XJ, Paul PS, Morozov I, Halbur PG.** 1996. A nested set of six or seven  
762 subgenomic mRNAs is formed in cells infected with different isolates of porcine  
763 reproductive and respiratory syndrome virus. *J Gen Virol* **77 ( Pt 6)**:1265-1270.
- 764 16. **Meulenberg JJ, Petersen-den Besten A.** 1996. Identification and characterization of a  
765 sixth structural protein of Lelystad virus: the glycoprotein GP2 encoded by ORF2 is  
766 incorporated in virus particles. *Virology* **225**:44-51.
- 767 17. **Snijder EJ, van Tol H, Pedersen KW, Raamsman MJ, de Vries AA.** 1999.  
768 Identification of a novel structural protein of arteriviruses. *J Virol* **73**:6335-6345.
- 769 18. **Wu WH, Fang Y, Farwell R, Steffen-Bien M, Rowland RR, Christopher-Hennings J,**  
770 **Nelson EA.** 2001. A 10-kDa structural protein of porcine reproductive and respiratory  
771 syndrome virus encoded by ORF2b. *Virology* **287**:183-191.
- 772 19. **Johnson CR, Griggs TF, Gnanandarajah J, Murtaugh MP.** 2011. Novel structural  
773 protein in porcine reproductive and respiratory syndrome virus encoded by an alternative  
774 ORF5 present in all arteriviruses. *J Gen Virol* **92**:1107-1116.
- 775 20. **Li Y, Tas A, Sun Z, Snijder EJ, Fang Y.** 2014. Proteolytic processing of the porcine  
776 reproductive and respiratory syndrome virus replicase. *Virus Res.*
- 777 21. **Fang Y, Treffers EE, Li Y, Tas A, Sun Z, van der Meer Y, de Ru AH, van Veelen**  
778 **PA, Atkins JF, Snijder EJ, Firth AE.** 2012. Efficient -2 frameshifting by mammalian  
779 ribosomes to synthesize an additional arterivirus protein. *Proc Natl Acad Sci U S A*  
780 **109**:E2920-2928.
- 781 22. **Chen Z, Lawson S, Sun Z, Zhou X, Guan X, Christopher-Hennings J, Nelson EA,**  
782 **Fang Y.** 2010. Identification of two auto-cleavage products of nonstructural protein 1  
783 (nsp1) in porcine reproductive and respiratory syndrome virus infected cells: nsp1  
784 function as interferon antagonist. *Virology* **398**:87-97.
- 785 23. **Beura LK, Sarkar SN, Kwon B, Subramaniam S, Jones C, Pattnaik AK, Osorio FA.**  
786 2010. Porcine reproductive and respiratory syndrome virus nonstructural protein 1beta  
787 modulates host innate immune response by antagonizing IRF3 activation. *J Virol*  
788 **84**:1574-1584.
- 789 24. **Kim O, Sun Y, Lai FW, Song C, Yoo D.** 2010. Modulation of type I interferon  
790 induction by porcine reproductive and respiratory syndrome virus and degradation of  
791 CREB-binding protein by non-structural protein 1 in MARC-145 and HeLa cells.  
792 *Virology* **402**:315-326.
- 793 25. **Li Y, Treffers EE, Naphine S, Tas A, Zhu L, Sun Z, Bell S, Mark BL, van Veelen**  
794 **PA, van Hemert MJ, Firth AE, Brierley I, Snijder EJ, Fang Y.** 2014. Transactivation  
795 of programmed ribosomal frameshifting by a viral protein. *Proc Natl Acad Sci U S A*  
796 **111**:E2172-2181.
- 797 26. **Li Y, Zhu L, Lawson SR, Fang Y.** 2013. Targeted mutations in a highly conserved  
798 motif of the nsp1beta protein impair the interferon antagonizing activity of porcine  
799 reproductive and respiratory syndrome virus. *J Gen Virol* **94**:1972-1983.
- 800 27. **Zeman D, Neiger R, Yaeger M, Nelson E, Benfield D, Leslie-Steen P, Thomson J,**  
801 **Miskimins D, Daly R, Minehart M.** 1993. Laboratory investigation of PRRS virus  
802 infection in three swine herds. *J Vet Diagn Invest* **5**:522-528.
- 803 28. **Fuerst TR, Niles EG, Studier FW, Moss B.** 1986. Eukaryotic transient-expression  
804 system based on recombinant vaccinia virus that synthesizes bacteriophage T7 RNA  
805 polymerase. *Proc Natl Acad Sci U S A* **83**:8122-8126.

- 806 29. **Nelson EA, Christopher-Hennings J, Drew T, Wensvoort G, Collins JE, Benfield**  
807 **DA.** 1993. Differentiation of U.S. and European isolates of porcine reproductive and  
808 respiratory syndrome virus by monoclonal antibodies. *J Clin Microbiol* **31**:3184-3189.
- 809 30. **Reed LJ, Muench H.** 1938. A simple method of estimating fifty per cent endpoints.  
810 *American journal of epidemiology* **27**:493-497.
- 811 31. **Fang Y, Rowland RR, Roof M, Lunney JK, Christopher-Hennings J, Nelson EA.**  
812 2006. A full-length cDNA infectious clone of North American type 1 porcine  
813 reproductive and respiratory syndrome virus: expression of green fluorescent protein in  
814 the Nsp2 region. *J Virol* **80**:11447-11455.
- 815 32. **Halbur PG, Paul PS, Frey ML, Landgraf J, Eernisse K, Meng XJ, Lum MA,**  
816 **Andrews JJ, Rathje JA.** 1995. Comparison of the pathogenicity of two US porcine  
817 reproductive and respiratory syndrome virus isolates with that of the Lelystad virus. *Vet*  
818 *Pathol* **32**:648-660.
- 819 33. **Binjawadagi B, Dwivedi V, Manickam C, Ouyang K, Torrelles JB, Renukaradhya**  
820 **GJ.** 2014. An innovative approach to induce cross-protective immunity against porcine  
821 reproductive and respiratory syndrome virus in the lungs of pigs through adjuvanted  
822 nanotechnology-based vaccination. *Int J Nanomedicine* **9**:1519-1535.
- 823 34. **Renukaradhya GJ, Alekseev K, Jung K, Fang Y, Saif LJ.** 2010. Porcine reproductive  
824 and respiratory syndrome virus-induced immunosuppression exacerbates the  
825 inflammatory response to porcine respiratory coronavirus in pigs. *Viral Immunol* **23**:457-  
826 466.
- 827 35. **Garcia-Iglesias T, Del Toro-Arreola A, Albarran-Somoza B, Del Toro-Arreola S,**  
828 **Sanchez-Hernandez PE, Ramirez-Duenas MG, Balderas-Pena LM, Bravo-Cuellar A,**  
829 **Ortiz-Lazareno PC, Daneri-Navarro A.** 2009. Low NKp30, NKp46 and NKG2D  
830 expression and reduced cytotoxic activity on NK cells in cervical cancer and precursor  
831 lesions. *BMC Cancer* **9**:186.
- 832 36. **Lecoeur H, Fevrier M, Garcia S, Riviere Y, Gougeon ML.** 2001. A novel flow  
833 cytometric assay for quantitation and multiparametric characterization of cell-mediated  
834 cytotoxicity. *J Immunol Methods* **253**:177-187.
- 835 37. **Dwivedi V, Manickam C, Patterson R, Dodson K, Murtaugh M, Torrelles JB,**  
836 **Schlesinger LS, Renukaradhya GJ.** 2011. Cross-protective immunity to porcine  
837 reproductive and respiratory syndrome virus by intranasal delivery of a live virus vaccine  
838 with a potent adjuvant. *Vaccine* **29**:4058-4066.
- 839 38. **Talker SC, Kaser T, Reutner K, Sedlak C, Mair KH, Koinig H, Graage R,**  
840 **Viehmann M, Klingler E, Ladinig A, Ritzmann M, Saalmuller A, Gerner W.** 2013.  
841 Phenotypic maturation of porcine NK- and T-cell subsets. *Dev Comp Immunol* **40**:51-68.
- 842 39. **Sinkora M, Butler JE.** 2009. The ontogeny of the porcine immune system. *Dev Comp*  
843 *Immunol* **33**:273-283.
- 844 40. **Zuckermann FA, Husmann RJ.** 1996. Functional and phenotypic analysis of porcine  
845 peripheral blood CD4/CD8 double-positive T cells. *Immunology* **87**:500-512.
- 846 41. **Denyer MS, Wileman TE, Stirling CM, Zuber B, Takamatsu HH.** 2006. Perforin  
847 expression can define CD8 positive lymphocyte subsets in pigs allowing phenotypic and  
848 functional analysis of natural killer, cytotoxic T, natural killer T and MHC un-restricted  
849 cytotoxic T-cells. *Vet Immunol Immunopathol* **110**:279-292.
- 850 42. **Costers S, Lefebvre DJ, Goddeeris B, Delputte PL, Nauwynck HJ.** 2009. Functional  
851 impairment of PRRSV-specific peripheral CD3+CD8high cells. *Vet Res* **40**:46.

- 852 43. **Dwivedi V, Manickam C, Patterson R, Dodson K, Weeman M, Renukaradhya GJ.**  
853 2011. Intranasal delivery of whole cell lysate of Mycobacterium tuberculosis induces  
854 protective immune responses to a modified live porcine reproductive and respiratory  
855 syndrome virus vaccine in pigs. *Vaccine* **29**:4067-4076.
- 856 44. **Kamijuku H, Nagata Y, Jiang X, Ichinohe T, Tashiro T, Mori K, Taniguchi M, Hase**  
857 **K, Ohno H, Shimaoka T, Yonehara S, Odagiri T, Tashiro M, Sata T, Hasegawa H,**  
858 **Seino KI.** 2008. Mechanism of NKT cell activation by intranasal coadministration of  
859 alpha-galactosylceramide, which can induce cross-protection against influenza viruses.  
860 *Mucosal Immunol* **1**:208-218.
- 861 45. **Guillonneau C, Mintern JD, Hubert FX, Hurt AC, Besra GS, Porcelli S, Barr IG,**  
862 **Doherty PC, Godfrey DI, Turner SJ.** 2009. Combined NKT cell activation and  
863 influenza virus vaccination boosts memory CTL generation and protective immunity.  
864 *Proc Natl Acad Sci U S A* **106**:3330-3335.
- 865 46. **Albina E, Piriou L, Hutet E, Cariolet R, L'Hospitalier R.** 1998. Immune responses in  
866 pigs infected with porcine reproductive and respiratory syndrome virus (PRRSV). *Vet*  
867 *Immunol Immunopathol* **61**:49-66.
- 868 47. **Van Reeth K, Labarque G, Nauwynck H, Pensaert M.** 1999. Differential production  
869 of proinflammatory cytokines in the pig lung during different respiratory virus infections:  
870 correlations with pathogenicity. *Res Vet Sci* **67**:47-52.
- 871 48. **Buddaert W, Van Reeth K, Pensaert M.** 1998. In vivo and in vitro interferon (IFN)  
872 studies with the porcine reproductive and respiratory syndrome virus (PRRSV). *Adv Exp*  
873 *Med Biol* **440**:461-467.
- 874 49. **Miller LC, Laegreid WW, Bono JL, Chitko-McKown CG, Fox JM.** 2004. Interferon  
875 type I response in porcine reproductive and respiratory syndrome virus-infected MARC-  
876 145 cells. *Arch Virol* **149**:2453-2463.
- 877 50. **Luo R, Xiao S, Jiang Y, Jin H, Wang D, Liu M, Chen H, Fang L.** 2008. Porcine  
878 reproductive and respiratory syndrome virus (PRRSV) suppresses interferon-beta  
879 production by interfering with the RIG-I signaling pathway. *Mol Immunol* **45**:2839-2846.
- 880 51. **Donelan NR, Basler CF, Garcia-Sastre A.** 2003. A recombinant influenza A virus  
881 expressing an RNA-binding-defective NS1 protein induces high levels of beta interferon  
882 and is attenuated in mice. *J Virol* **77**:13257-13266.
- 883 52. **Talon J, Salvatore M, O'Neill RE, Nakaya Y, Zheng H, Muster T, Garcia-Sastre A,**  
884 **Palese P.** 2000. Influenza A and B viruses expressing altered NS1 proteins: A vaccine  
885 approach. *Proc Natl Acad Sci U S A* **97**:4309-4314.
- 886 53. **Valarcher JF, Furze J, Wyld S, Cook R, Conzelmann KK, Taylor G.** 2003. Role of  
887 alpha/beta interferons in the attenuation and immunogenicity of recombinant bovine  
888 respiratory syncytial viruses lacking NS proteins. *J Virol* **77**:8426-8439.
- 889 54. **Zust R, Cervantes-Barragan L, Kuri T, Blakqori G, Weber F, Ludewig B, Thiel V.**  
890 2007. Coronavirus non-structural protein 1 is a major pathogenicity factor: implications  
891 for the rational design of coronavirus vaccines. *PLoS Pathog* **3**:e109.
- 892 55. **Frias-Staheli N, Giannakopoulos NV, Kikkert M, Taylor SL, Bridgen A, Paragas J,**  
893 **Richt JA, Rowland RR, Schmaljohn CS, Lenschow DJ, Snijder EJ, Garcia-Sastre A,**  
894 **Virgin HWt.** 2007. Ovarian tumor domain-containing viral proteases evade ubiquitin-  
895 and ISG15-dependent innate immune responses. *Cell Host Microbe* **2**:404-416.

- 896 56. **Sun Z, Chen Z, Lawson SR, Fang Y.** 2010. The cysteine protease domain of porcine  
897 reproductive and respiratory syndrome virus nonstructural protein 2 possesses  
898 deubiquitinating and interferon antagonism functions. *J Virol* **84**:7832-7846.
- 899 57. **Sun Z, Li Y, Ransburgh R, Snijder EJ, Fang Y.** 2012. Nonstructural protein 2 of  
900 porcine reproductive and respiratory syndrome virus inhibits the antiviral function of  
901 interferon-stimulated gene 15. *J Virol* **86**:3839-3850.
- 902 58. **van Kasteren PB, Bailey-Elkin BA, James TW, Ninaber DK, Beugeling C,**  
903 **Khajehpour M, Snijder EJ, Mark BL, Kikkert M.** 2013. Deubiquitinase function of  
904 arterivirus papain-like protease 2 suppresses the innate immune response in infected host  
905 cells. *Proc Natl Acad Sci U S A* **110**:E838-847.
- 906 59. **Manickam C, Dwivedi V, Patterson R, Papenfuss T, Renukaradhya GJ.** 2013.  
907 Porcine reproductive and respiratory syndrome virus induces pronounced immune  
908 modulatory responses at mucosal tissues in the parental vaccine strain VR2332 infected  
909 pigs. *Vet Microbiol* **162**:68-77.
- 910 60. **Schroder K, Hertzog PJ, Ravasi T, Hume DA.** 2004. Interferon-gamma: an overview  
911 of signals, mechanisms and functions. *J Leukoc Biol* **75**:163-189.
- 912 61. **De Bruin TG, Van Rooij EM, De Visser YE, Bianchi AT.** 2000. Cytolytic function for  
913 pseudorabies virus-stimulated porcine CD4+ CD8dull+ lymphocytes. *Viral Immunol*  
914 **13**:511-520.
- 915 62. **Franzoni G, Kurkure NV, Essler SE, Pedrera M, Everett HE, Bodman-Smith KB,**  
916 **Crooke HR, Graham SP.** 2013. Proteome-wide screening reveals immunodominance in  
917 the CD8 T cell response against classical swine fever virus with antigen-specificity  
918 dependent on MHC class I haplotype expression. *PLoS One* **8**:e84246.
- 919 63. **Takamatsu HH, Denyer MS, Lacasta A, Stirling CM, Argilaguet JM, Netherton CL,**  
920 **Oura CA, Martins C, Rodriguez F.** 2013. Cellular immunity in ASFV responses. *Virus*  
921 *Res* **173**:110-121.
- 922 64. **Binjawadagi B, Dwivedi V, Manickam C, Ouyang K, Wu Y, Lee LJ, Torrelles JB,**  
923 **Renukaradhya GJ.** 2014. Adjuvanted poly(lactic-co-glycolic) acid nanoparticle-  
924 entrapped inactivated porcine reproductive and respiratory syndrome virus vaccine elicits  
925 cross-protective immune response in pigs. *Int J Nanomedicine* **9**:679-694.
- 926 65. **Wang S, Fan Y, Brunham RC, Yang X.** 1999. IFN-gamma knockout mice show Th2-  
927 associated delayed-type hypersensitivity and the inflammatory cells fail to localize and  
928 control chlamydial infection. *Eur J Immunol* **29**:3782-3792.
- 929 66. **Song Z, Wu H, Ciofu O, Kong KF, Hoiby N, Rygaard J, Kharazmi A, Mathee K.**  
930 2003. *Pseudomonas aeruginosa* alginate is refractory to Th1 immune response and  
931 impedes host immune clearance in a mouse model of acute lung infection. *J Med*  
932 *Microbiol* **52**:731-740.
- 933 67. **Diaz MA, Villalobos N, de Aluja A, Rosas G, Gomez-Conde E, Hernandez P,**  
934 **Larralde C, Sciutto E, Fragoso G.** 2003. Th1 and Th2 indices of the immune response  
935 in pigs vaccinated against *Taenia solium* cysticercosis suggest various host immune  
936 strategies against the parasite. *Vet Immunol Immunopathol* **93**:81-90.

937

938

939

940 **FIGURE LEGEND**

941 **Figure 1.** Mutations in GKYLQRRLQ motif impair nsp1 $\beta$ 's inhibitory effect on type I interferon  
942 production and signaling. HEK-293T cells in 24-well plate were co-transfected with a plasmid  
943 expressing WT nsp1 $\beta$  or nsp1 $\beta$  mutant, p125-luc reporter plasmid expressing firefly luciferase  
944 under the control of IFN- $\beta$  promoter (**A**) or pISRE-luc expressing firefly luciferase derived by  
945 interferon stimulated response element (ISRE; **B**). Empty vector was used as control. At 24 h  
946 post-transfection, cells were stimulated with SeV at 100 HA units/ml or stimulated with IFN- $\beta$  at  
947 2000 IU/ml for 16 h. Cell lysates were harvested for measuring luciferase activity. (**C**) The  
948 expression level of nsp1 $\beta$  was evaluated by western blot analysis using nsp1 $\beta$ -specific mAb 123-  
949 128, whereas  $\beta$ -tubulin was detected as a loading control. The membrane was incubated with  
950 primary antibodies mixture of anti-FLAG M2 mAb (Sigma-Aldrich, St. Louis, MO) and mAb  
951 against  $\beta$ -tubulin. Secondary antibody IRDye® 800CW Goat anti-Mouse IgG (H + L) (LI-COR  
952 Biosciences, Lincoln, NE) was used for visualizing the target proteins with a digital image  
953 system (Odyssey infrared imaging system; LI-COR Biosciences, Lincoln, NE). The expression  
954 of nsp1 $\beta$  was quantified and normalized to  $\beta$ -tubulin, and the relative expression levels were  
955 showed under each band. Statistical significance between wild type group and mutant virus  
956 group was determined by one-way ANOVA and Tukey's test, and indicated with asterisk (\*,  
957  $p < 0.05$ ; \*\*,  $p < 0.01$ ; \*\*\*,  $p < 0.001$ ).

958 **Figure 2.** Mutations at R128 and R129 in GKYLQRRLQ motif impair the expression of nsp2TF  
959 in vaccinia/T7 expression system. HEK-293T cells were infected with vaccinia virus expressing  
960 T7 polymerase at 10 MOI, and then transfected with pLnsp1 $\beta$ -2 constructs at 1 h post-infection.  
961 The cell lysates were harvested at 18 h post-transfection. (**A**) The nsp2TF was  
962 immunoprecipitated by polyclonal antibody (pAb-TF) that specifically recognizes the C-terminal

963 region of nsp2TF using equal amount of lysate. Immunoprecipitated proteins were detected by  
964 WB using pAb-TF (top panel) and mAb 140-68 recognizing the common N-terminal region of  
965 nsp2-related proteins (bottom panel); **(B)** Western blot detecting the expression of nsp2 (top  
966 panel), nsp1 $\beta$  (bottom panel) using specific mAbs.

967 **Figure 3.** *In vitro* characterization of recombinant viruses containing nsp1 $\beta$  mutations. **(A)**  
968 Multiple-step virus growth curve. Each data point shown represents a mean value from  
969 duplicates, and error bars show standard errors of the mean (SEM). **(B)** Plaque morphology of  
970 WT and recombinant viruses containing mutations in the GKYLQRRLQ motif of nsp1 $\beta$ .

971 **Figure 4.** Mutations in GKYLQRRLQ motif attenuate the ability of PRRSV to suppress the  
972 expression of IFN- $\alpha$  and ISGs. Porcine alveolar macrophages seeded in 24-well plate were  
973 infected with the WT virus or nsp1 $\beta$  mutants at a MOI of 1.0, and cell culture supernatants were  
974 harvested at 12 h post-infection. **(A)** IFN- $\alpha$  production was quantified by using ProcartaPlex  
975 Porcine IFN alpha Simplex kit (eBioscience, San Diego, CA). Each data point shown represents  
976 a mean value from three independent experiments with duplicate, and error bars show SEM. **(B)**  
977 The mRNA expression of ISG15 was evaluated by quantitative real-time PCR and normalized to  
978 endogenous  $\beta$ -tubulin mRNA. **(C)** The mRNA expression of IFIT1 was evaluated by quantitative  
979 real-time PCR and normalized to endogenous  $\beta$ -tubulin mRNA. **(D)** The mRNA expression of  
980 IFITM1 was evaluated by quantitative real-time PCR and normalized to endogenous  $\beta$ -tubulin  
981 mRNA. Values (B, C, and D) are expressed as the means  $\pm$  SEM from three independent  
982 experiments. **(E)** The expression of nsp1 $\beta$  at 12 h post-infection was determined by western blot  
983 analysis with nsp1 $\beta$ -specific mAb 123-128, whereas  $\beta$ -tubulin was detected as a loading control.  
984 The membrane was incubated with primary antibodies mixture of mAb123-128 and mAb against  
985  $\beta$ -tubulin. Secondary antibody IRDye® 800CW Goat anti-Mouse IgG (H + L) (LI-COR

986 Biosciences, Lincoln, NE) was used for visualizing the target proteins with a digital image  
987 system (Odyssey infrared imaging system; LI-COR Biosciences, Lincoln, NE). Statistical  
988 significance between wild type group and mutant virus group was determined by one-way  
989 ANOVA and Tukey's test, and indicated with asterisk (\*,  $p < 0.05$ ; \*\*,  $p < 0.01$ ; \*\*\*,  $p < 0.001$ ).

990 **Figure 5.** Comparison of viral load in serum samples from pigs inoculated with WT virus and  
991 nsp1 $\beta$  mutants. Pigs were uninfected (mock), infected with WT PRRSV (WT), or three indicated  
992 mutants (vR128A, vR129A, vRR129AA). Serum samples were collected on the indicated DPIs.

993 **(A)** Viral load in serum samples quantified by quantitative RT-PCR and calculated as viral RNA  
994 copies/ml. **(B)** Infectious virus titer in serum samples determined by micro-titration assay and  
995 calculated as logTCID<sub>50</sub>/ml. Statistical significance between wild type group and mutant virus  
996 group was determined by one-way ANOVA and Tukey's test, and indicated with asterisk (\*,  
997  $p < 0.05$ ; \*\*,  $p < 0.01$ ; \*\*\*,  $p < 0.001$ ).

998 **Figure 6.** Comparison of viral load in BALF and lung samples from pigs inoculated with WT  
999 virus and nsp1 $\beta$  mutants. Pigs were uninfected (mock), infected with WT PRRSV (WT), or three  
1000 indicated mutants (vR128A, vR129A, vRR129AA). The lung harvested on the day of necropsy  
1001 (7, 21 and 35 DPI) was used in BALF and lung lysate preparation. **(A and B)** Viral load in  
1002 BALF **(A)** and lung lysate **(B)** samples was quantified by quantitative RT-PCR and calculated as  
1003 viral RNA copies/ml BALF or viral RNA copies/g lung. **(C and D)** Infectious virus titer in  
1004 BALF **(C)** and lung lysate **(D)** samples was determined by micro-titration assay and calculated as  
1005 logTCID<sub>50</sub>/ml or logTCID<sub>50</sub>/g. A legend explaining the treatment groups in panels **(B)**, **(C)**, and  
1006 **(D)** is given in panel **(A)**. Statistical significance between wild type group and mutant virus  
1007 group was determined by one-way ANOVA and Tukey's test, and indicated with asterisk (\*,  
1008  $p < 0.05$ ; \*\*,  $p < 0.01$ ; \*\*\*,  $p < 0.001$ ).



1009 **Figure 7.** Comparison of IFN- $\alpha$  production levels and NK cell cytotoxicity in pigs inoculated  
1010 with WT virus and nsp1 $\beta$  mutants. Pigs were uninfected (mock), infected with WT PRRSV  
1011 (WT), or three indicated mutants (vR128A, vR129A, vRR129AA). **(A)** The lung samples  
1012 collected at 7 DPI were used to prepare lung lysates, and IFN- $\alpha$  levels were analyzed by ELISA.  
1013 **(B and C)** PBMCs (NK effectors) were harvested on the day of necropsy (7 DPI), and cells were  
1014 co-cultured with target cells (K562) at E:T ratio of 100:1**(B)** or 50:1**(C)**. After overnight  
1015 incubation, the NK specific cytotoxic activity was determined by flow cytometry. Each data  
1016 point represents a mean value  $\pm$  SEM from 3 pigs. Statistical significance between wild type  
1017 group and mutant virus group was determined by one-way ANOVA and Tukey's test, and  
1018 indicated with asterisk (\*,  $p < 0.05$ ; \*\*,  $p < 0.01$ ; \*\*\*,  $p < 0.001$ ).

1019 **Figure 8.** Comparison of IFN- $\gamma$  production levels in pigs inoculated with WT virus and nsp1 $\beta$   
1020 mutants. Pigs were uninfected (mock), infected with WT PRRSV (WT), or three indicated  
1021 mutants (vR128A, vR129A, vRR129AA). Blood samples were collected on the indicated DPIs,  
1022 and the BALF and lung lysate were prepared using lungs harvested on the day of necropsy (7, 21  
1023 and 35 DPI). IFN $\gamma$  levels in **(A)** Serum and **(B)** Lung lysate, and IL-6 levels in **(C)** BALF and  
1024 **(D)** Lung lysate were analyzed by ELISA. Each data point represents a mean value  $\pm$  SEM from  
1025 3 pigs. Statistical significance between wild type group and mutant virus group was determined  
1026 by one-way ANOVA and Tukey's test, and indicated with asterisk (\*,  $p < 0.05$ ; \*\*,  $p < 0.01$ ; \*\*\*,  
1027  $p < 0.001$ ).

1028 **Figure 9.** T-helper and Memory T cells responses in pigs infected with nsp1 $\beta$  mutants. PBMCs  
1029 collected at 7, 21 and 35 DPI were unstimulated or restimulated with the respective WT or  
1030 mutant viruses that were used to infect pigs. Cells were immunostained for pig specific markers

1031 CD3, CD4, and CD8 $\alpha$ , followed by intracellular IFN- $\gamma$  detection. Frequency of each lymphocyte  
1032 subset based on the combination of markers are grouped: **(A)** CD3<sup>+</sup>CD4<sup>-</sup>CD8 $\alpha$ <sup>+</sup> (CTL/ $\gamma\delta$  T  
1033 cells); **(B)** CD3<sup>+</sup>CD4<sup>-</sup>CD8 $\alpha$ <sup>+</sup>IFN $\gamma$ <sup>+</sup> (activated CTL/ $\gamma\delta$  T cells); **(C)** CD3<sup>+</sup>CD4<sup>+</sup>CD8 $\alpha$ <sup>+</sup> (T-  
1034 helper/Memory cells); **(D)** CD3<sup>+</sup>CD4<sup>+</sup>CD8 $\alpha$ <sup>+</sup>IFN $\gamma$ <sup>+</sup> (activated T-helper/Memory cells) and **(E)**  
1035 CD3<sup>-</sup>CD8 $\alpha$ <sup>+</sup>IFN $\gamma$ <sup>+</sup> (activated NK cells) were analyzed by flow cytometry. A legend explaining  
1036 the treatment groups in panels **(A)**, **(B)**, **(D)**, and **(E)** is given in panel **(C)**. Each bar is the mean  
1037 value  $\pm$  SEM of 3 pigs. Statistical significance between wild type and mutant virus-infected pig  
1038 groups was determined by one-way ANOVA and followed by Tukey's t-test, and indicated with  
1039 asterisk (\*, p<0.05; \*\*, p<0.01; \*\*\*, p<0.001).

**Table 1.** Experimental design for testing of nsp1 $\beta$  mutants in nursery pigs

	dpi	Pig Number				
		Negative control (group 1)	WT <sup>e</sup> (group 2)	R128A (group 3)	R129A (group 4)	RR129AA (group 5)
<b>Blood collection<sup>a</sup></b>	0	1 ~ 9 <sup>c</sup>	10 ~ 18	19 ~ 27	28 ~ 36	37 ~ 45
	1	1 ~ 9	10 ~ 18	19 ~ 27	28 ~ 36	37 ~ 45
	2	1 ~ 9	10 ~ 18	19 ~ 27	28 ~ 36	37 ~ 45
	5	1 ~ 9	10 ~ 18	19 ~ 27	28 ~ 36	37 ~ 45
	14	4 ~ 9	14 ~ 18	22 ~ 27	31 ~ 36	40 ~ 45
	28	7 ~ 9	17, 18	25 ~ 27	34 ~ 36	43 ~ 45
<b>Animal termination<sup>b</sup></b>	7	1 ~ 3 <sup>d</sup>	10, 11, 13	19 ~ 21	28 ~ 30	37 ~ 39
	21	4 ~ 6	14 ~ 16	22 ~ 24	31 ~ 33	40 ~ 42
	35	7 ~ 9	17, 18	25 ~ 27	34 ~ 36	43 ~ 45

**a:** At 0, 1, 2, 5, 14, and 28 dpi, plasma and PBMCs were collected;

**b:** At 7, 21, and 35 dpi, 3 pigs from each group were terminated, and their plasma, PBMCs, bronchoalveolar lavage fluid and lung tissue samples were collected;

**c:** Pigs for blood collection at indicated time point;

**d:** Pigs terminated at indicated time point;

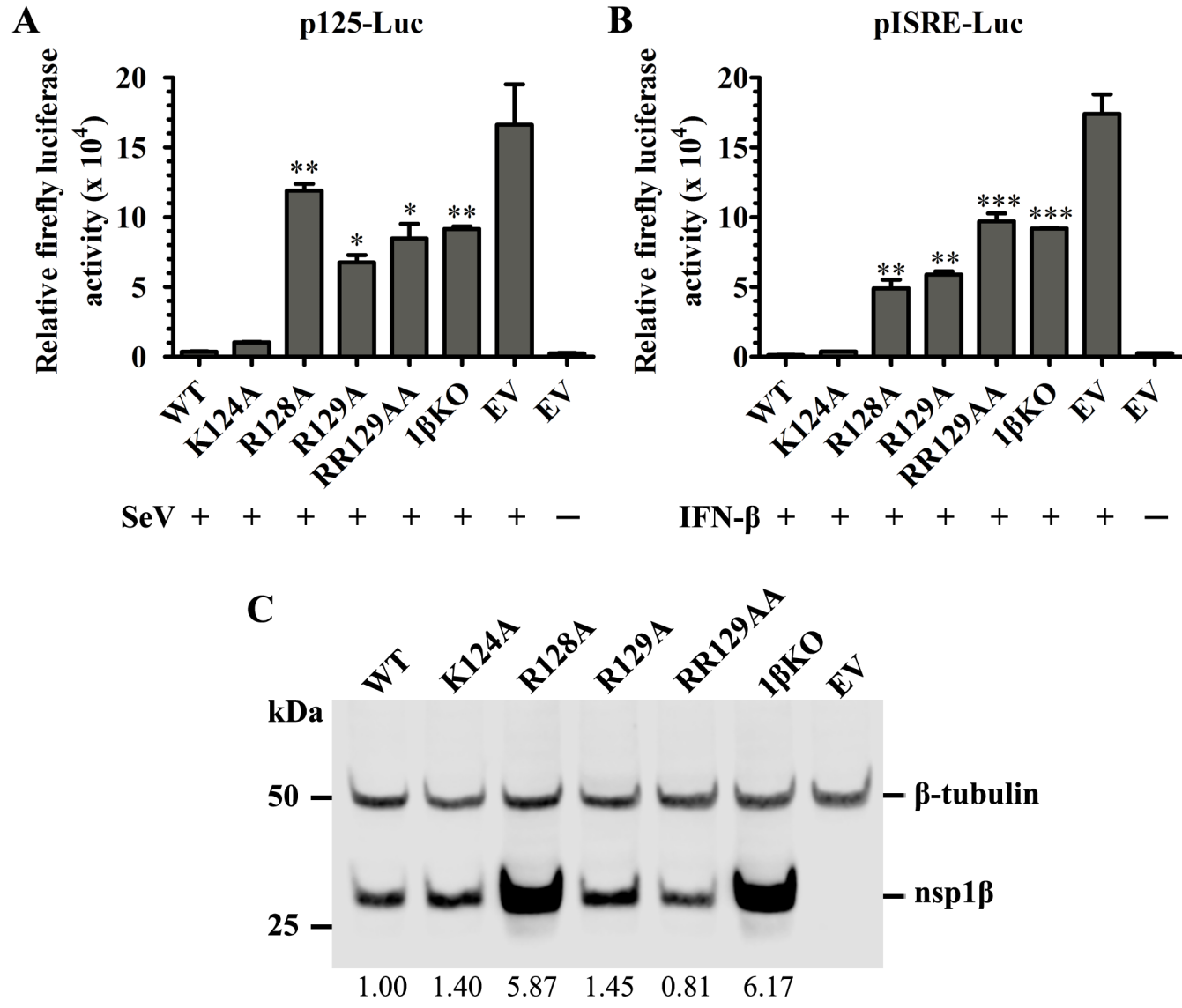
**e:** Pig #12 died before 7 dpi

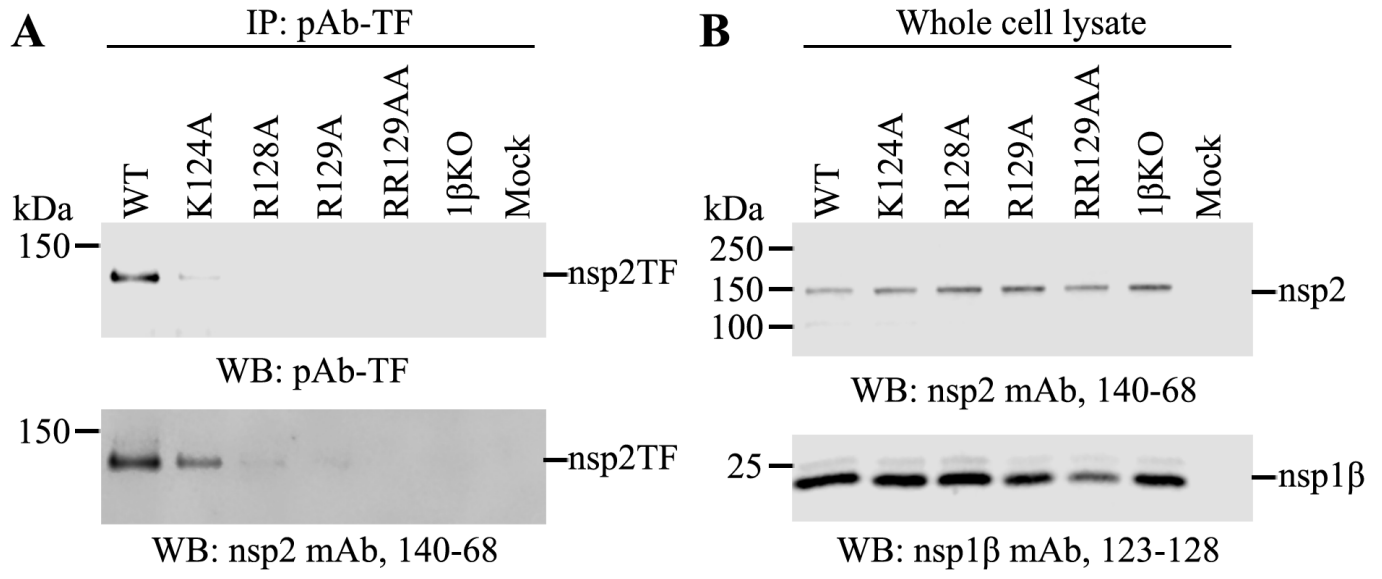
**Table 2.** Sequence analysis of nsp1 $\beta$  coding region in viruses recovered from infected pigs

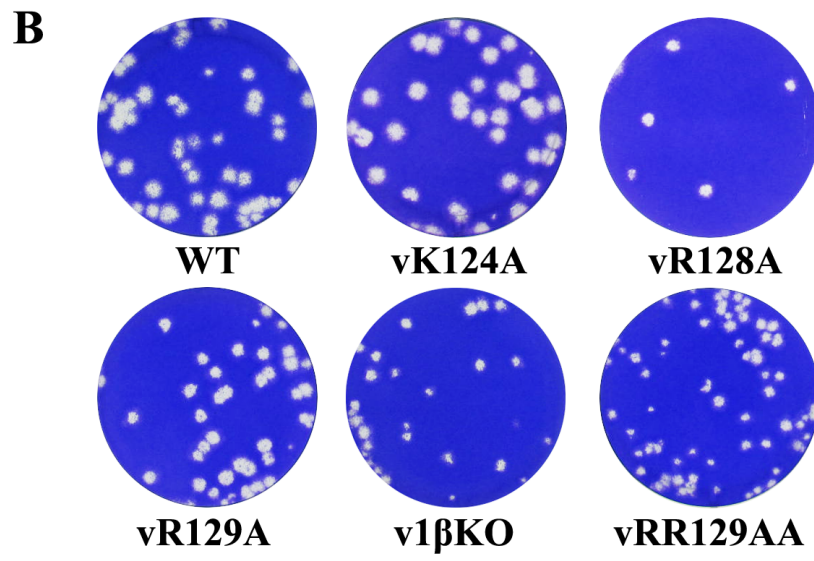
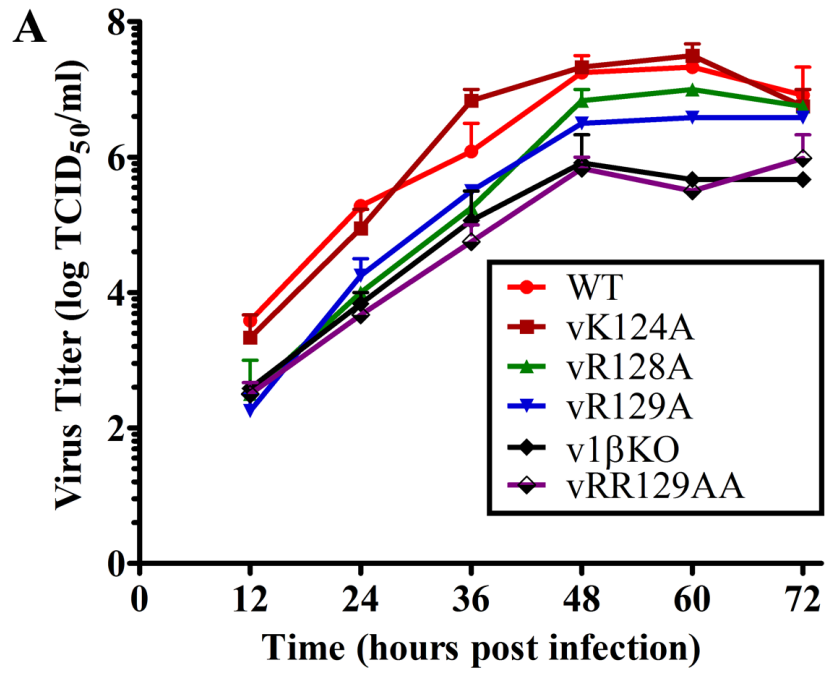
Group	Pig #	Designed Mutation	2 <sup>nd</sup> site Mutation
<b>14 days post infection</b>			
vR129A	31	reversion (GCG to AGG)	
	32	stable	122 <sup>a</sup> : UCU to CCU <sup>b</sup> , Ser to Pro <sup>c</sup>
	33	stable	122: UCU to CCU, Ser to Pro
	34	stable	122: UCU to CCU, Ser to Pro
	35	stable	122: UCU to CCU, Ser to Pro
	36	stable	122: UCU to CCU, Ser to Pro
<b>21 days post infection</b>			
WT	14		9: GAC to GGC, Asp to Gly
	15		9: GAC to GGC, Asp to Gly
	16		9: GAC to GGC, Asp to Gly
vR128A	22	stable	9: GAC to GGC, Asp to Gly; 122: UCU to CCU, Ser to Pro
	23	stable	9: GAC to GGC, Asp to Gly; 122: UCU to CCU, Ser to Pro
	24	stable	9: GAC to GGC, Asp to Gly; 109: CAU to C(A/G)U, His to His/Arg; 122: UCU to CCU, Ser to Pro; 141: CUA to C(U/C)A, Leu to Leu/Pro
vR129A	31	reversion (GCG to AGG)	9: GAC to GGC, Asp to Gly
	32	stable	9: GAC to GGC, Asp to Gly; 87: GAA to GA(A/G); 122: UCU to CCU, Ser to Pro
	33	stable	9: GAC to GGC, Asp to Gly; 122: UCU to CCU, Ser to Pro; 169: UCU to (C/U)CU, Ser to Ser/Pro
vRR129AA	40	stable	
	41	stable	
	42	stable	
<b>35 days post infection</b>			
WT	17		9: GAC to GGC, Asp to Gly; 126: CUA to CU(A/G)
	18		9: GAC to GGC, Asp to Gly
vR128A	27	stable	9: GAC to GGC, Asp to Gly; 109: CAU to CGU, His to Arg; 122: UCU to CCU, Ser to Pro
vR129A	34	stable	9: GAC to GGC, Asp to Gly; 122: UCU to CCU, Ser to Pro; 132: UUU to (G/U)UU, Phe to Val;

vR129A	34		141: CUA to CU(A/G) 169: UCU to (C/U)CU, Ser to Ser/Pro
	35	stable	9: GAC to GGC, Asp to Gly; 122: UCU to CCU, Ser to Pro;
	36	stable	9: GAC to GGC, Asp to Gly; 122: UCU to CCU, Ser to Pro; 169: UCU to CCU, Ser to Pro
vRR129AA	44	stable	9: GAC to GGC, Asp to Gly
	45	stable	9: GAC to GGC, Asp to Gly

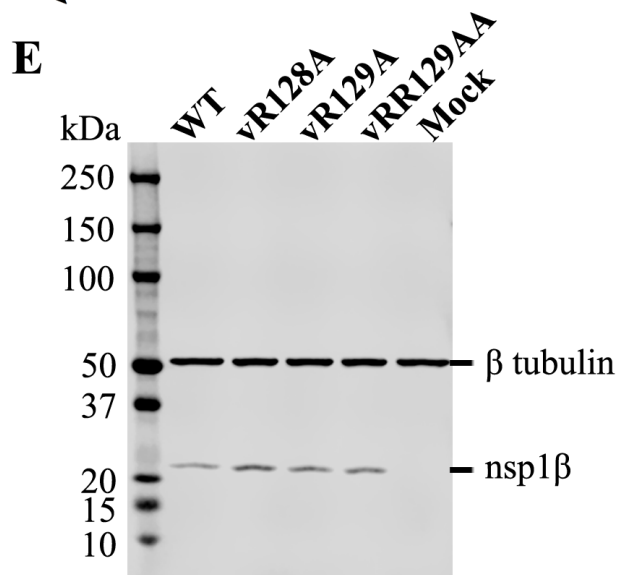
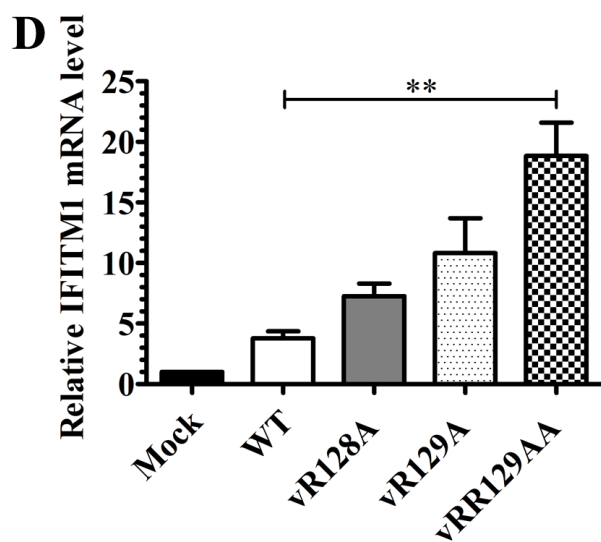
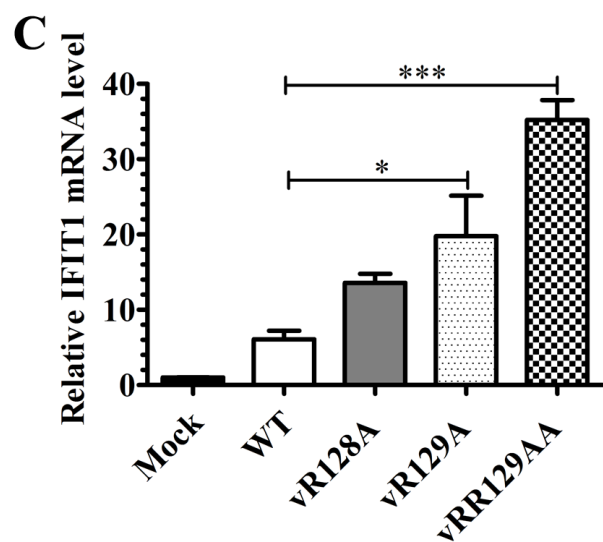
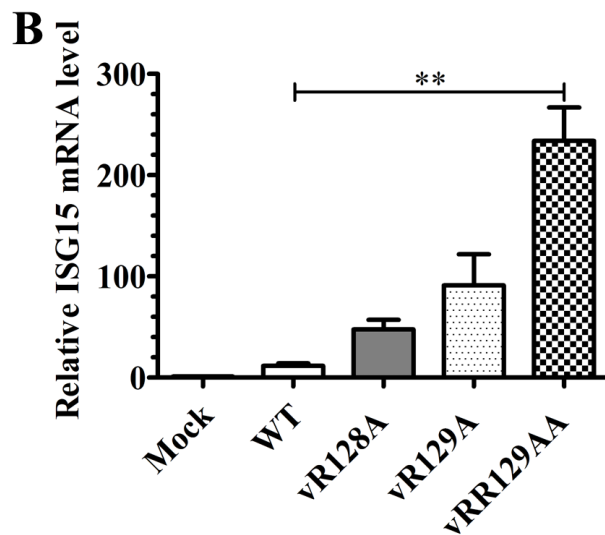
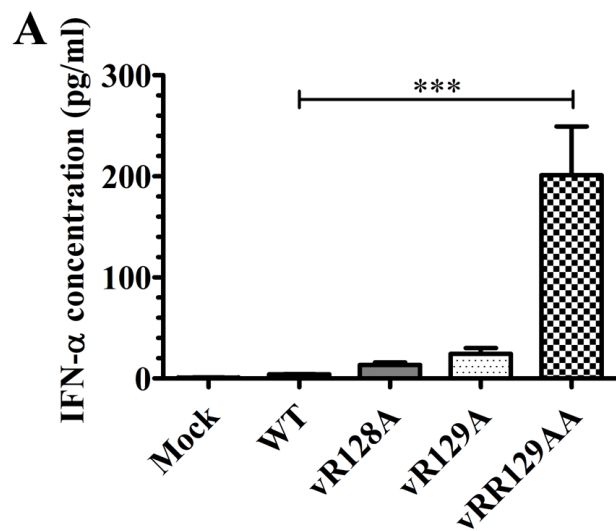
a. Numbers refer to codon position in nsp1 $\beta$  coding region; b. Nucleotide substitution; c. Amino acid substitution.











WB: nsp1 $\beta$  mAb, 123-128;  $\alpha$ - $\beta$  tubulin

